The role of microRNA alterations in post-ischemic neovascularization

Kwast, R.V.C.T. van der

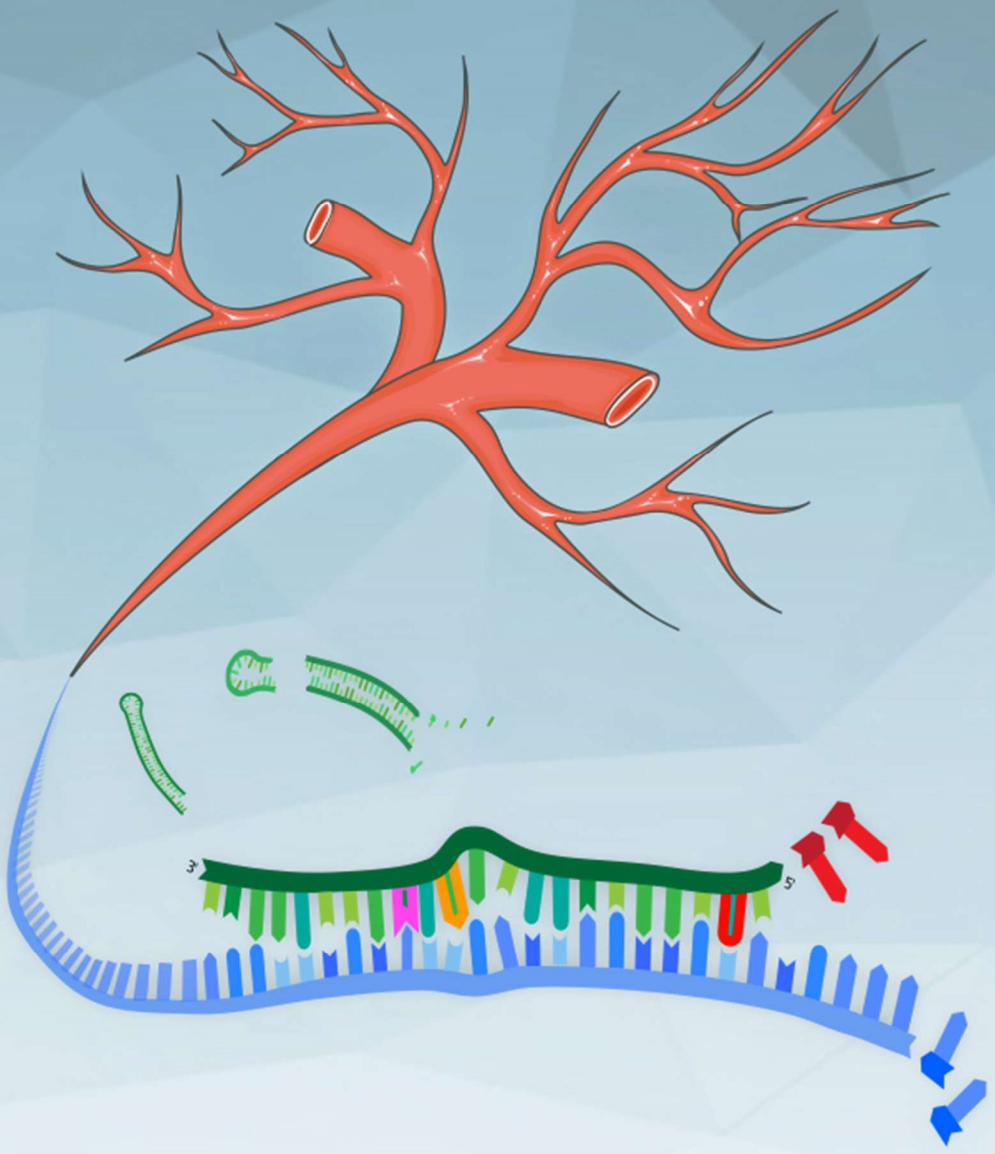
3'
5'

CHAPTER 3

MicroRNA-411 and its 5'-isomiR have distinct targets and functions and are differentially regulated in the vasculature under ischemia

Reginald V.C.T. van der Kwast
Tamar Woudenberg
Paul H.A. Quax
A. Yaël Nossent

Molecular Therapy. 2020 Jan 8;28(1):157-170

ABSTRACT

MicroRNAs are posttranscriptional regulators of gene expression. As microRNAs can target many genes simultaneously, microRNAs can regulate complex multifactorial processes, including post-ischemic neovascularization, a major recovery pathway in cardiovascular disease. MicroRNAs select their target mRNAs via full-complementary binding with their seed-sequence, i.e. nucleotides 2-8 from the 5'-end of a microRNA. The exact sequence of a mature microRNA, and thus of its 5'- and 3'- ends, is determined by two sequential cleavage steps of microRNA precursors, by Drosha/DGCR8 and Dicer. When these cleavage steps result in nucleotide switches at the 5'-end, forming a so-called 5'-isomiR, this results in a shift in the mature microRNA's seed-sequence. The role of 5'-isomiRs in cardiovascular diseases is still unknown.

Here we characterize the expression and function of the 5'-isomiR of miR-411 (ISO-miR-411). ISO-miR-411 is abundantly expressed in human primary vascular cells. ISO-miR-411 has a different 'targetome' from WT-miR-411, with only minor overlap. The ISO-miR-411/WT-miR-411 ratio is downregulated under acute ischemia, both in cells and a murine ischemia model, but is upregulated instead in chronically ischemic human blood vessels. ISO-miR-411 negatively influences vascular cell migration, whereas WT-miR-411 does not. Our data demonstrate that isomiR formation is a functional pathway that is actively regulated during ischemia.

Keywords: microRNA, isomiR, cardiovascular disease, ischemia, angiogenesis, microRNA biogenesis, DROSHA

INTRODUCTION

MicroRNAs are ~22 nt-long small noncoding RNAs that regulate a wide range of physiological and pathological processes, including processes controlling cardiovascular function.[2-5] MicroRNAs are able to inhibit translation of protein coding transcripts (mRNAs). A single microRNA can target hundreds of mRNAs, often regulating an entire network or pathway simultaneously.[6] The microRNA's "seed" sequence, nucleotides 2 to 8 from the 5'-end of the microRNA, predominantly determines target site recognition.[7,8]

The 5'- and 3'-ends of a microRNA are determined during the maturation steps of the primary transcript of the microRNA gene, known as the pri-miRNA.[9,10] First the pri-miRNA is cleaved in the nucleus by the Microprocessor complex composed of ribonuclease (RNase) III enzyme DROSHA and DGCR8 to generate a hairpin-shaped precursor miRNA (pre-miRNA).[11] The pre-miRNA is exported to the cytoplasm where it is processed further by RNase III enzyme DICER into a microRNA duplex.[12] The separate strands of the duplex can be incorporated into the RNA-induced silencing complex (RISC) as functional mature microRNAs.[13]

Typically, microRNAs are annotated as a single defined sequence, and are listed as such in the principle public microRNA database, miRBase.[14] However, deep sequencing studies have revealed that for many microRNAs, sequence variants with slightly different 5′- and/or 3′-ends, known as isomiRs, can be generated from a single pri-miRNA hairpin.[15] This type of 5′ and 3′ heterogeneity derives from variations in processing by the DROSHA and/or DICER enzymes.[16-18] These isomiRs have been shown to function like canonical microRNAs, since they associate actively both with the RISC and with translational machinery polysomes.[10,19-21] IsomiRs with 5′-end variations, or 5'-isomiRs, are expected to be functionally important as they result in an altered seed sequence, i.e. nucleotides 2 to 8 from the 5'-end, compared to the canonical microRNA, and are therefore expected to display altered target site selection. IsomiRs can have tissue specific expression and their expression profiles alone allow for discrimination between cancer types.[21-23] These observations suggest that isomiRs, and 5'-isomiRs in particular, can play an independent role in regulating pathophysiological processes. However, the specific roles of individual isomiRs and when they are regulated remain largely unknown.

MicroRNAs play a key role in cardiovascular disease.[4,5,24] Although cardiovascular diseases have a complex, multifactorial pathology, ischemia plays an intricate part in both the development and manifestation of most cardiovascular diseases. In response to ischemia, the adaptive growth of blood vessels, known as neovascularization, helps to restore blood flow. We have shown that the microRNAs from a large microRNA gene cluster located on the long arm of human chromosome 14 (14q32) are regulated during ischemia in mice and can directly affect neovascularization.[25] Interestingly, recent studies have shown that one of these 14q32 microRNAs, miR-411, has a 5'-isomiR.[26] This miR-411 5'-isomiR (ISO-miR-41) has an additional 5' adenosine compared to the canonical 'wildtype' miR-411 (WT-miR-411). The isomiR appears to be the result of a single nucleotide shift in DROSHA's cleavage of the primary miR-411 transcript (pri-miR-411) (**Figure 1A**). Currently however, the prevalence, regulation and function of ISO-miR-411 is unknown.

In this study we demonstrate that ISO-miR-411 is at least 5-fold more abundant than WT-miR-411 in primary human vascular cells and in venous tissue samples from patients with peripheral artery disease (PAD). Additionally, we show that ISO-miR-411 and WT-miR-411 expression is differentially regulated in cultured vascular fibroblasts under ischemic conditions and we confirm these findings in a murine hindlimb ischemia model. Finally, we demonstrate that ISO-miR-411 indeed targets a different and larger set of genes than WT-miR-411, resulting in functional differences in angiogenesis *in vitro*.

RESULTS

Prevalence of ISO-miR-411

We analyzed public microRNA-sequencing (miRNA-seq) datasets to examine the prevalence of ISO-miR-411 relative to WT-miR-411 in human and murine tissues. The miRNA-seq data showed that ISO-miR-411 is expressed in all examined tissues. ISO-miR-411 expression relative to WT-miR-411 expression varied strongly per tissue (**Figure 1B&C**). For example, in both human and murine datasets the ratio of ISO-miR-411 over WT-miR-411 (ISO/WT-miR-411) was below 0.5 skin tissue while the ratio was approximately 4 in cardiac tissue. Furthermore, ISO/WT-miR-411 is decreased in datasets from murine whole body tissue of 9.5 days old embryos, 12.5 days old embryos

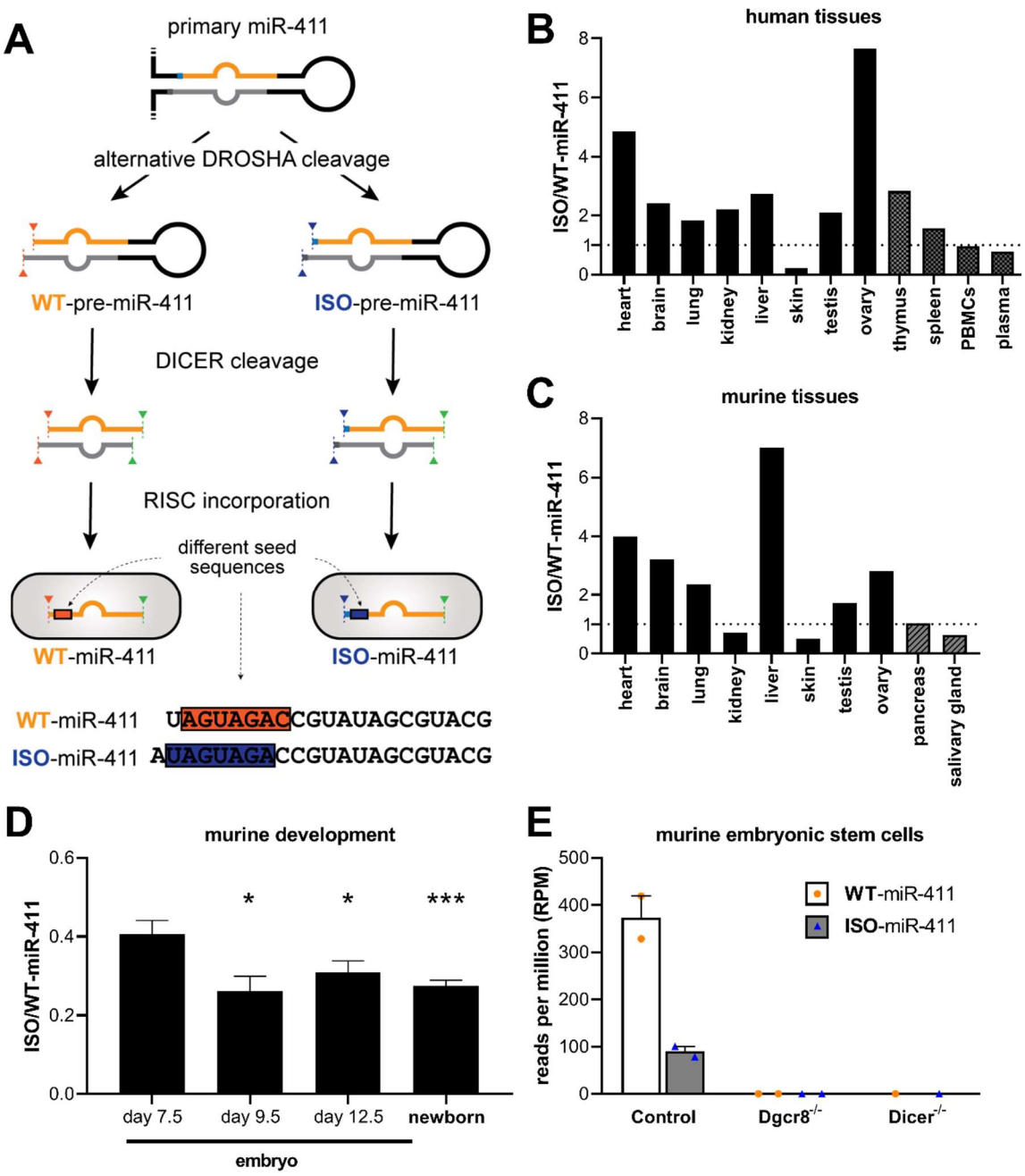

Figure 1: **Biogenesis and expression of miR-411 and its 5'-isomiR.** (A) The biogenesis of canonical 'wildtype' miR-411 (WT-miR-411) and its 5'-isomiR (ISO-miR-411). Endonuclease DROSHA can cleave the primary miR-411 transcript at 2 distinct locations, which results in 2 different precursor microRNAs, WT-pre-miR-411 or ISO-pre-miR-411. Mature WT-miR-411 and ISO-miR-411 are produced after their respective pre-miRNAs and preferential incorporation into the RISC complex. Compared to WT-miR-411, ISO-miR-411 has an additional nucleotide at its 5'-end (in blue) and therefore has a different seed sequence. (B-D) Public microRNA-seq datasets were analyzed to examine the prevalence of ISO-miR-411 relative to WT-miR-411 in human tissues (B, n=1) murine tissues (C, n=1) and during murine development (D, n≥4). (E) Expression of WT-miR-411 and ISO-miR-411 in public microRNA-seq data from control murine embryonic stem cells and murine embryonic stem cells with a knockout of either *Dgcr8* (*Dgcr8*$^{-/-}$) or *Dicer* (*Dicer*$^{-/-}$) (n=1 or 2). (D-E) Data are presented as mean ±SEM. *P<0.05, ***P<0.001; versus embryos of day 7.5 by 2-sided Student t test.

and newborn mice when compared to 7.5 days old embryos (ISO/WT-miR-411 0.26±0.04, 0.31±0.03 and 0.27±0.01 versus 0.41±0.03, *P*<0.03, *P*<0.05 and *P*<0.001, respectively) (**Figure 1D**). These observations suggest that WT-miR-411 and ISO-miR-411 expression are differentially regulated over time. Both WT-miR-411 and ISO-miR-411 were confirmed to be products of the microRNA maturation pathway, since both their expression is abolished in murine embryonic stem cells deficient for either Dgcr8 or Dicer (**Figure 1E**).

WT-miR-411 and ISO-miR-411 expression in vascular cells

We then determined whether ISO-miR-411 is also abundantly expressed in primary human umbilical arterial fibroblasts (HUAFs) and human umbilical venous endothelial cells (HUVECs). Expression of WT-miR-411 and ISO-miR-411 were quantified using 5' Dumbbell-Polymerase-Chain-Reaction (5'DB-PCR), specifically designed and validated to distinguish between the highly similar sequences of WT-mir-411 and ISO-miR-411 (**Supplemental Figure I**). We found that ISO-miR-411 is expressed at least 5-fold higher than WT-miR-411 in both cell types (**Figure 2A**). However, the expression of both WT-mir-411 and ISO-miR-411 was approximately 3-fold higher in HUAFs compared to HUVECs (**Figure 2A**, *P*=0.02 and *P*=0.07 respectively). Therefore, subsequent experiments were performed in HUAFs.

We then cultured HUAFs under ischemic conditions to examine whether miR-411 expression is regulated under ischemia. Both 24h and 48h of ischemic culture conditions successfully induced hypoxic signaling and cell cycle arrest, as demonstrated by increased expression of *HIF1A*, *VEGFA* and *SDF1*, and *p53* respectively (**Supplemental Figure II**). After 24h of ischemia,

WT-miR-411 expression increased by 3.3-fold while ISO-miR-411 expression increased by only 1.6-fold (**Figure 2B**, upper panel, *P*=0.01 and *P*=0.03 versus control, respectively), decreasing ISO/WT-miR-411 from 6.4±1.0 under control conditions to 3.2±0.4 after 24h of ischemia (bottom panel, *P*=0.04). After 48h ischemic conditions, both WT-miR-411 and ISO-miR-411 expression decreased again (upper panel, *P*=0.08 and *P*<0.05 versus 24h, respectively), but ISO/WT-miR-411 remained decreased (bottom panel, 48h ratio: 3.9±0.3; *P*=0.08). These data demonstrate that mature WT-miR-411 and ISO-miR-411 are differentially regulated under ischemia in human primary vascular fibroblasts.

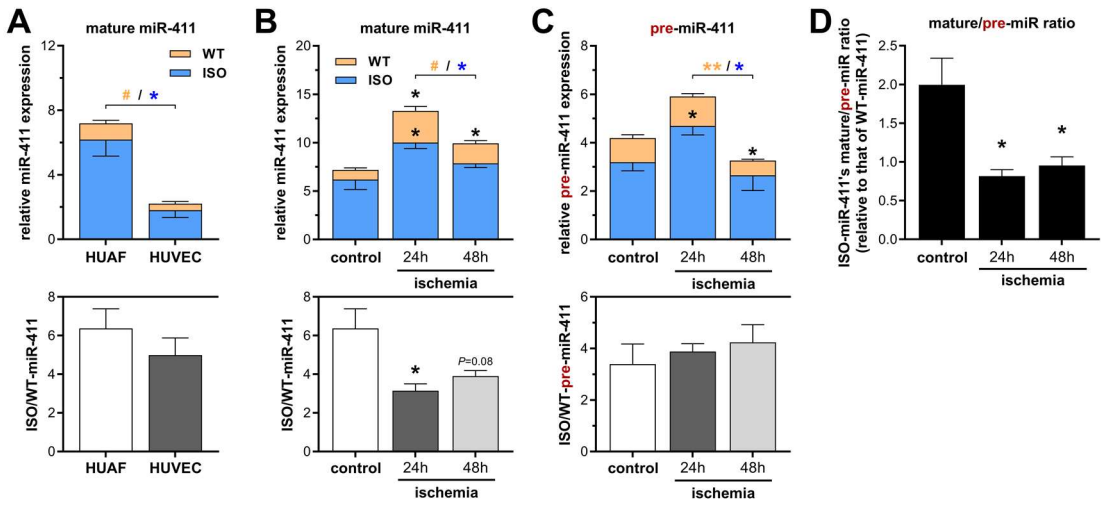

Figure 2: **WT-miR-411 and ISO-miR-411 expression in primary vascular cells under ischemic conditions.** (A-C) 5'-Dumbbell-PCR was used to quantify WT-miR-411 (white) from ISO-miR-411 (dark gray) transcripts. In each graph, relative expression is presented in the upper panel while the corresponding ISO/WT-miR-411 ratio is shown in the bottom panel. (A) WT-miR-411 and ISO-miR-411 expression in human umbilical venous endothelial cells (HUVECs) and human umbilical arterial fibroblasts (HUAFs). (B-C) Regulation of mature miR-411 expression (B) and pre-miR-411 expression (C) and their respective ISO/WT ratios after subjecting HUAFs to ischemic conditions for 24h or 48h. Ischemic conditions were induced by a combination of hypoxia and serum starvation, resulting in hypoxia signaling and cell cycle arrest (**Supplemental Figure II**). MiR-411 expression was normalized to U6 and presented as fold of WT-miR-411 expression in the HUAF control group. (D) The mature/pre-miR ratio of ISO-miR-411 relative to the WT-miR-411's mature/pre-miR ratio as calculated from data in panels B and C. All data are shown as mean ±SEM (n=3). #P<0.1, *P<0.05, **P<0.01; versus control condition unless otherwise indicated by 2-sided Student t test.

WT-pre-miR-411 and ISO-pre-miR-411 expression

To determine at which step in the microRNA processing WT-miR-411 and ISO-miR-411 are regulated, we also quantified 'wildtype' pre-miR-411 (WT-pre-miR-411) and isomiR pre-miR-411 (ISO-pre-miR-411) expression using 5'DB-PCR. Similar to mature miRNA levels, ISO-pre-miR-411 expression was higher than WT-pre-miR-411 expression in primary arterial fibroblasts and followed a similar pattern under ischemic conditions: increased expression after 24h ischemia and subsequently decreased expression after 48h ischemia (**Figure 2C** upper panel). However, the ISO/WT-pre-miR-411 ratio did not decrease under ischemia and even appeared to increase slightly, although not statistically significant (**Figure 2C** lower panel). To examine if ISO-miR-411's mature and pre-miR levels are inversely correlated, we calculated the ISO-miR-

411's mature/pre-miR ratio relative to the WT-miR-411's mature/pre-miR ratio. The ratio is significantly decreased in fibroblasts grown under ischemia (**Figure 2D**). These results suggest that, while Drosha cleavage introduces differential expression between WT-pre-miR-411 and ISO-pre-miR-411, it is the final maturation step that induces differential expression of mature WT-miR-411 and ISO-miR-411 under ischemia.*Regulation of factors involved in miRNA biogenesis*

In agreement with previous studies, we observed downregulation of important components of the microRNA machinery under ischemic conditions, including *DROSHA* and *DICER* (**Figure 3A**).[27,28] *DROSHA* has several isoforms, 2 of which were upregulated under ischemia but still expressed at relatively low levels (**Figure 3B**). The dominant isoform on the other hand was modestly downregulated. Differential regulation of *DROSHA* isoforms is therefore unlikely to explain differential regulation of WT-miR-411 versus ISO-miR-411. The enzymes adenosine deaminase acting on RNA 1 (*ADAR1*) and *ADAR2* however, were upregulated under ischemia (**Figure 3C**), as was shown previously.[29,30] Although they were initially described to regulate RNA editing, both ADAR1 and ADAR2 have been shown to regulate microRNA processing.[30-32] Indeed when we specifically inhibit ADAR1 using siRNAs (**Supplemental Figure III**), both WT-miR-411 and ISO-miR-411 are downregulated (**Figure 3D**). Notably, both pre-miRNAs are upregulated, indicating that ADAR1 facilitates processing of both WT- and ISO-pre-miR-411 (**Figure 3E**). ADAR1 knockdown did not affect the ISO/WT-miR-411 ratios, indicating that ADAR1 does not selectively bind either isoform of miR-411.

WT-miR-411 and ISO-miR-411 expression in vivo

Next we examined WT-miR-411 and ISO-miR-411 expression in distinct whole-muscle tissues (adductor, gastrocnemius and soleus) of C57Bl/6 mice before and after induction of acute hindlimb ischemia (HLI). We observed differences in baseline miR-411 expression between the different muscles (**Figure 4A**). Consistent with our *in vitro* results, expression of both WT-miR-411 and ISO-miR-411 transiently increased in the ischemic gastrocnemius and soleus muscles 1 day (T1) after HLI compared to before surgery (T0). Also consistent with the *in vitro* data, the ISO/WT-miR-411 ratio decreased at both T1 and T3. The decrease in ISO/WT ratio was not observed at the pre-miR-411 stage in either ischemic muscles, which is also consistent with our *in vitro*

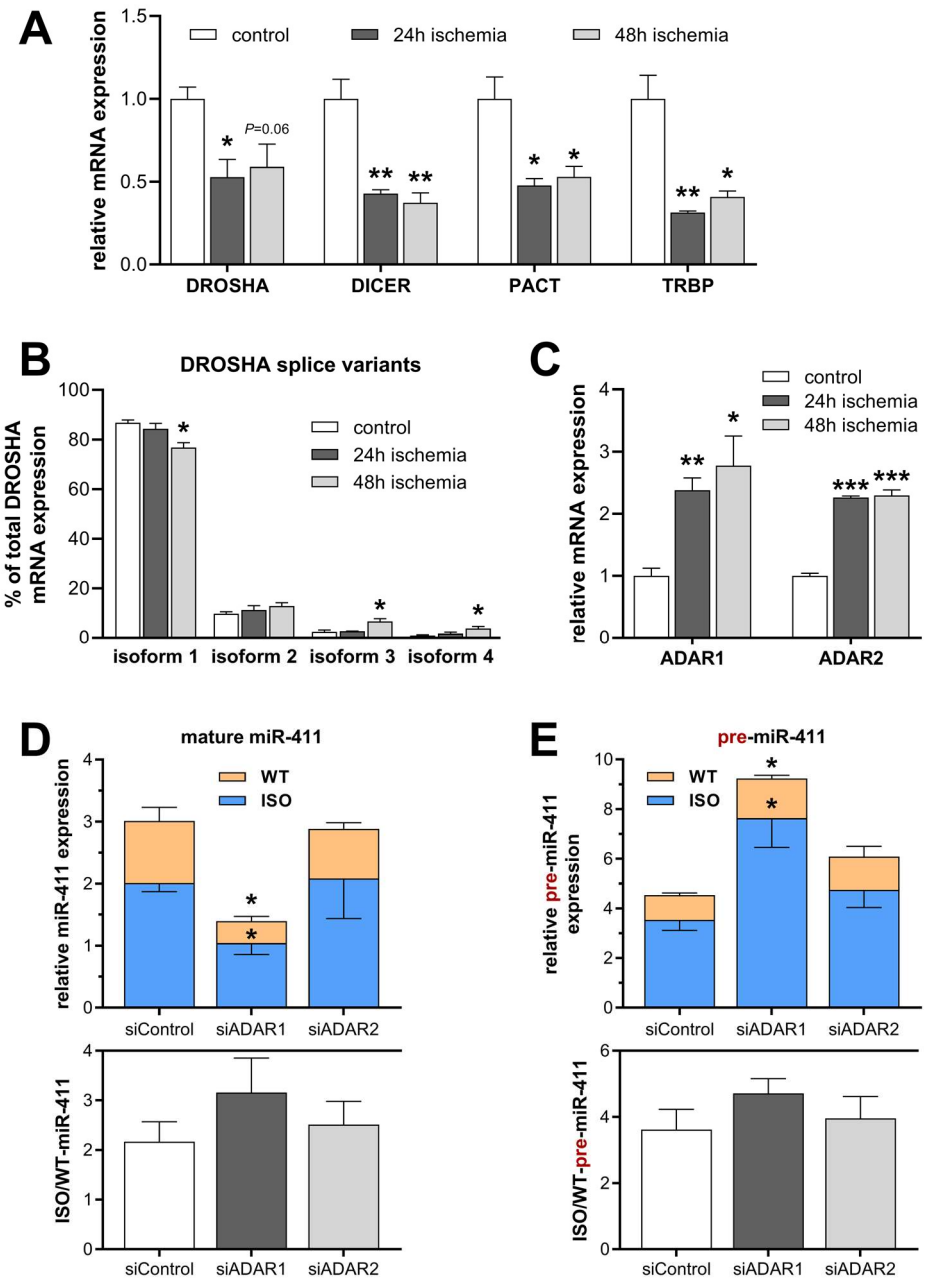

Figure 3: **Expression of microRNA biogenesis factors and the role of ADARs in miR-411 biogenesis.** (A) Expression of factors involved in microRNA biogenesis after culturing HUAFs under control or ischemic conditions, as quantified by qRT-PCR. (B) Relative expression of individual *DROSHA* isoforms as percentage of total *DROSHA* mRNA expression. (C) Expression of *ADAR1* and *ADAR2* in control or ischemic HUAFs quantified by qRT-PCR. (A-C) **P*<0.05, ***P*<0.01, ****P*<0.001; versus control condition by 2-sided Student *t* test. (D-E) ADAR1 and ADAR2 were knocked down in HUAFs through transfection of an *ADAR1*-targeting or *ADAR2*-targeting siRNA (siADAR1 and siADAR2 respectively). The subsequent effects on WT- and ISO-miR-411 expression (D) and WT- and ISO-pre-miR-411 expression (E) were determined as in **Figure 2** and compared to transfection with a negative control siRNA (siNegCtrl). (D-E) **P*<0.05 versus siNegCtrl by 2-sided Student *t* test. All data are presented as mean ± SEM (n=3).

results (**Figure 4B**). Furthermore, the ISO-miR-411's relative mature/pre-miR ratio was decreased at T3 in the ischemic gastrocnemius and soleus muscles, suggesting ISO-pre-miR-411 processing is also lowered after acute ischemia *in vivo* compared to processing of WT-pre-miR (**Figure 4C**). In this particular mouse model, the adductor remains relatively normoxic.[1] Accordingly, we did not observed changes in the ISO/WT-miR-411 ratios (**Figure 4A-C**). These results demonstrate that WT-miR-411 and ISO-miR-411 expression are also differentially regulated in response to ischemia *in vivo*.

WT-miR-411 and ISO-miR-411 expression in patients

To examine miR-411 expression in patients with chronic ischemia we measured the ISO/WT-miR-411 ratio in chronically ischemic lower leg vein (LLV) samples from patients with end-stage peripheral artery disease (PAD), undergoing lower limb amputation. We compared these to asymptomatic LLV samples from patients with coronary artery disease (CAD) undergoing coronary artery bypass-surgery. We found that ISO-miR-411 was more abundantly expressed than WT-miR-411 in all LLV samples. Furthermore, the ISO/WT-miR-411 ratio was 2.2-fold higher in the chronically ischemic LLV samples compared to the normoxic LLV samples (P=0.06) (**Figure 4D**). These data show that WT-miR-411 and ISO-miR-411 are also differentially expressed during chronic ischemia in humans, however, expression patterns clearly differ from those under acute ischemia.

In silico targetome predictions

The ISO-miR-411 has a seed sequence that is different from any other human microRNA seed-sequence (www.targetscan.org, release 7.2)[33] and will therefore have a unique targetome. To examine the differences between the targetomes of WT-miR-411 and ISO-miR-411 we used three distinct target prediction algorithms. We found that the targetome of ISO-miR-411 contains approximately twice as many putative target genes than the WT-miR-411 targetome (**Figure 5A**). The majority of putative target genes are unique to either the WT- or the ISO-miR-411 targetome (58% and 78% respectively). In fact, approximately half of the overlapping targets (129 of 269, 48%) are shared targets only because the mRNAs have independent binding sites for both WT-miR-411 and ISO-miR-411, rather than containing a single binding site that can be targeted by both WT-miR-411 and ISO-miR-411.

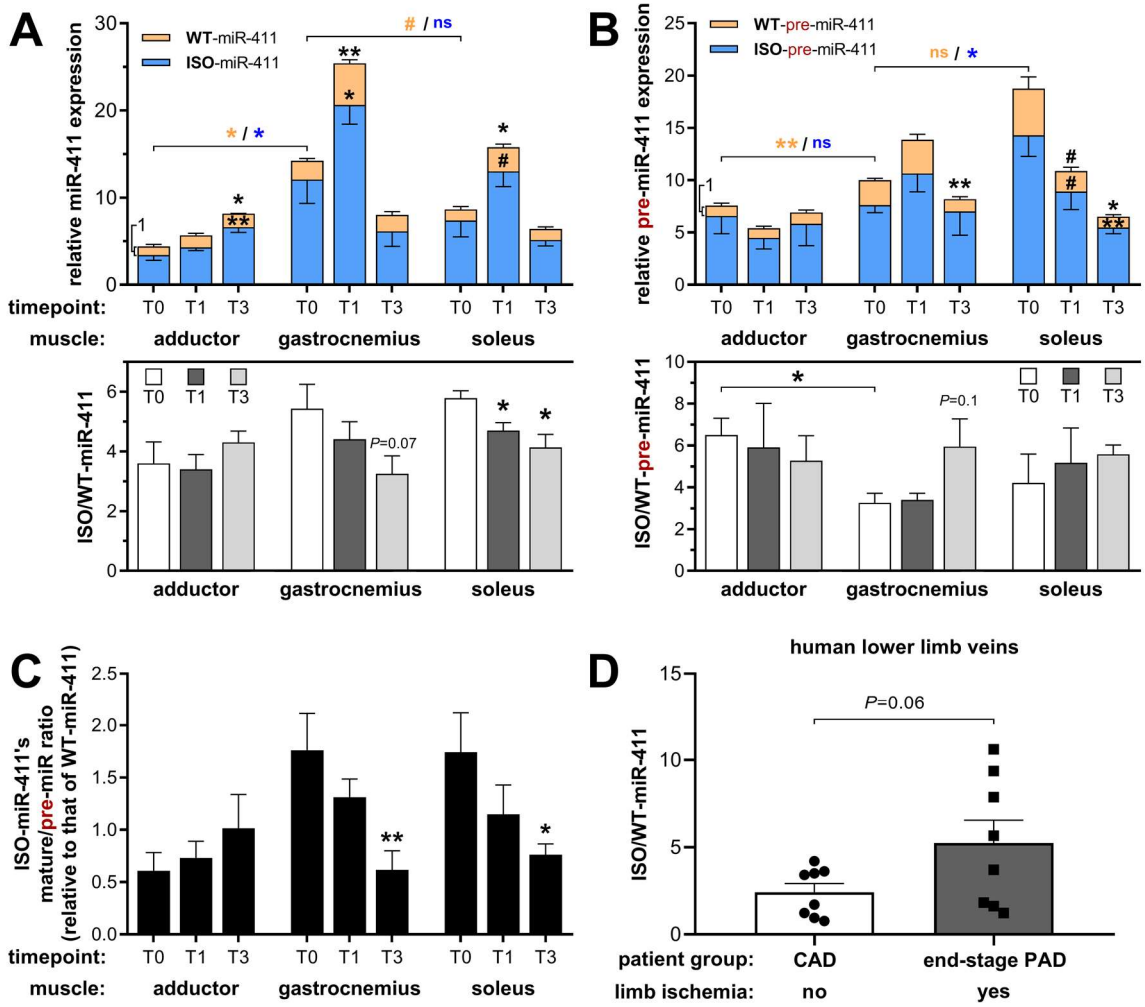

Figure 4: **MiR-411 regulation after acute hindlimb ischemia in mice and in human chronically ischemic lower limb veins.** (A-B) MiR-411 expression was measured by 5'-DB-PCR in three different mouse muscle tissues were harvested before (T0) or 1 and 3 days after induction of hindlimb ischemia (T1 and T3) (n=4 per group). While the gastrocnemius and soleus experience ischemia after surgery, the adductor remains relatively normoxic due to its more upstream anatomical location.[1] Regulation of mature miR-411 expression (A) and pre-miR-411 expression (B) and ISO-miR-411's relative mature/pre-miR ratio (C) after hindlimb ischemia, displayed as described in **Figure 2**. (D) ISO/WT-miR-411 ratio in lower leg vein (LLV) samples from normoxic LLV samples (n=8) from patients with coronary artery disease (CAD) compared to critically ischemic LLV samples (n=8) from patients with end-stage PAD, undergoing lower limb amputation. All data are presented as mean ± SEM. #P<0.1, *P<0.05, **P<0.01, ***P<0.001; versus T0 unless otherwise indicated by 2-sided Student t test. Symbol color shows whether means of WT or ISO expression are compared.

Pathway enrichment analyses of the targetomes using the PANTHER algorithm[34] revealed that both the WT-miR-411 and ISO-miR-411 targetomes contain overrepresentation of genes related to Cadherin signaling and Wnt signaling, most of which are shared targets (**Figure 5B** and **Supplemental Table I**).

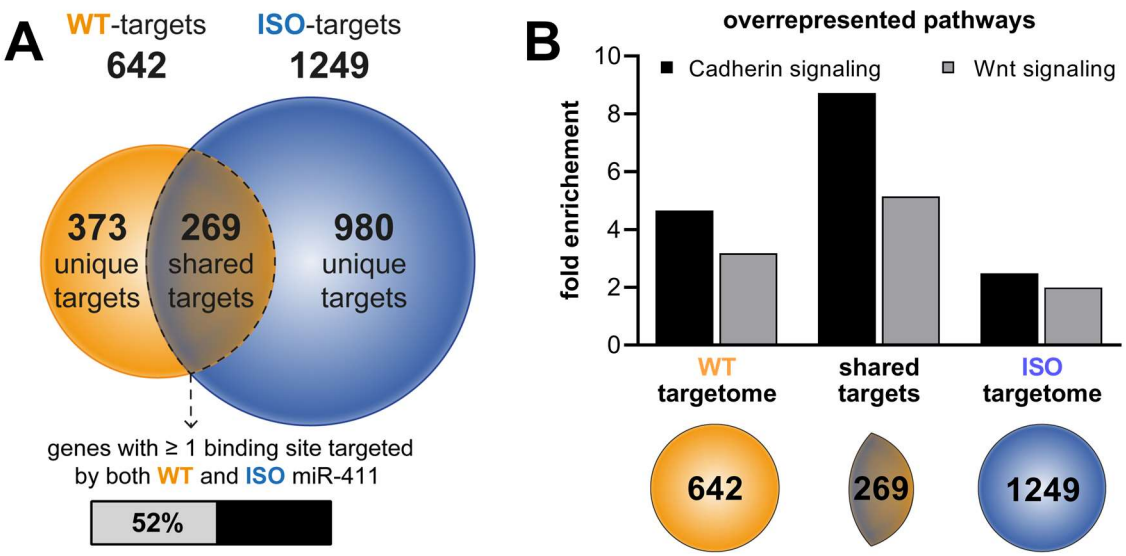

Figure 5: ***In silico* prediction of WT-miR-411 and ISO-miR-411 targetomes.** (A) Venn diagram of putative targetomes for WT-miR-411 (white) and ISO-miR-411 (dark gray) representing the putative target genes that were unanimously identified by all three employed prediction algorithms. (B) Significantly enriched pathways within the different targetomes and within the subset of shared targets (details in **Supplemental Table I**).

Validation of differential target regulation

In order to validate whether there are indeed WT-miR-411 specific targets, ISO-miR-411 specific targets and shared targets, we selected at least one gene from each target group that could be linked to the response to ischemia: transforming growth factor beta-2 (*TGFB2*, target of WT-miR-411), cadherin-2 (*CDH2*, shared target), cadherin-6 (*CDH6*, shared target), tissue factor (*F3*, target of ISO-miR-411) and angiopoietin-1 (*ANGPT1*, target of ISO-miR-411). MicroRNA-binding to these genes was examined by incorporating their endogenous 3'UTR putative binding sequences in luciferase reporter constructs and performing reporter gene assays (**Figure 6A**). Luciferase activity of the WT-miR-411 binding site-containing *TGFB2* sequence was indeed only repressed by WT-miR-411 to 89±1% (P=0.01) and not by ISO-miR-411 (P=0.5). Luciferase activity of sequences from shared targets *CDH2* and *CDH6* was reduced by both WT-miR-411 and ISO-miR-411. Finally, luciferase activity of ISO-miR-411 binding site-containing *F3* and *ANGPT1* sequences was repressed only by ISO-miR-411 to 85±2% (P=0.01) and 56±5% (P=0.01), respectively.

Next, we overexpressed either WT-miR-411 or ISO-miR-411 in HUAFs and examined endogenous target mRNA regulation (**Figure 6B**). Consistent with luciferase

results, treatment with WT-miR-411 decreased endogenous expression of *TGFB2*, *CDH2* and, to a lesser extent, *CDH6* by 43±9% (*P*=0.04), 28±5% (*P*=0.03) and 23±20% (*P*=0.3), respectively, but did not decrease *F3* or *ANGPT1* expression (*P*=0.5 and *P*=0.7). Conversely, treatment with ISO-miR-411 did not affect *TGFB2* expression (*P*=0.7), while expression of *CDH2*, *CDH6*, *F3* and *ANGPT1* were repressed by 40±5% (*P*=0.01), 30±10% (*P*=0.1), 28±6% (*P*=0.04) and 36±7% (*P*=0.03), respectively.

To confirm whether endogenous target mRNA regulation indeed results in regulation of protein levels, we selected TGFB2 as target for the WT-miR-411 and ANGPT1 as target for ISO-miR-411. No secretion of TGFB2 protein could be detected in the conditioned medium of our HUAFs (data not shown), but TGFB2 was detected in whole cell lysates (**Figure 6C**). Consistent with our findings on mRNA levels, TGFB2 protein was significantly downregulated after treatment with WT-miR-411 (*P*=0.04), but not after treatment with ISO-miR-411 (*P*=0.4). ANGPT1 is secreted by HUAFs and ANGPT1 levels in HUAF conditioned medium remained unaltered after treatment with WT-miR-411 (*P*=0.8), but were decreased after treatment with ISO-miR-411 (*P*=0.005) (**Figure 6D**). These results confirm that ISO-miR-411 has a unique targetome that only partially overlaps with the targetome of WT-miR-411.

Functional effects of miRNA editing

Functional effects of WT-miR-411 and ISO-miR-411 were examined by measuring HUAF cell migration using scratch-wound healing assays after overexpression of either microRNA. Changes in percentage ISO/WT-miR-411 ratio after microRNA overexpression were validated using 5'DB-PCR (**Supplemental Figure IV**). Treatment with ISO-miR-411 reduced wound healing by 24±3% (*P*=0.01) compared to the control microRNA treatment, while WT-miR-411 treatment did not (*P*=0.3) (**Figure 7**).

DISCUSSION

In this study we found that the 5'-isomiR of miR-411, ISO-miR-411, is more abundant than miR-411 itself (WT-miR-411) in primary human vascular fibroblasts and in human venous tissue samples. We demonstrate that ISO-miR-411 and WT-miR-411 expression are differentially regulated in response to ischemia *in vitro* as well as *in vivo* in a murine hindlimb ischemia model. We show that the observed differential

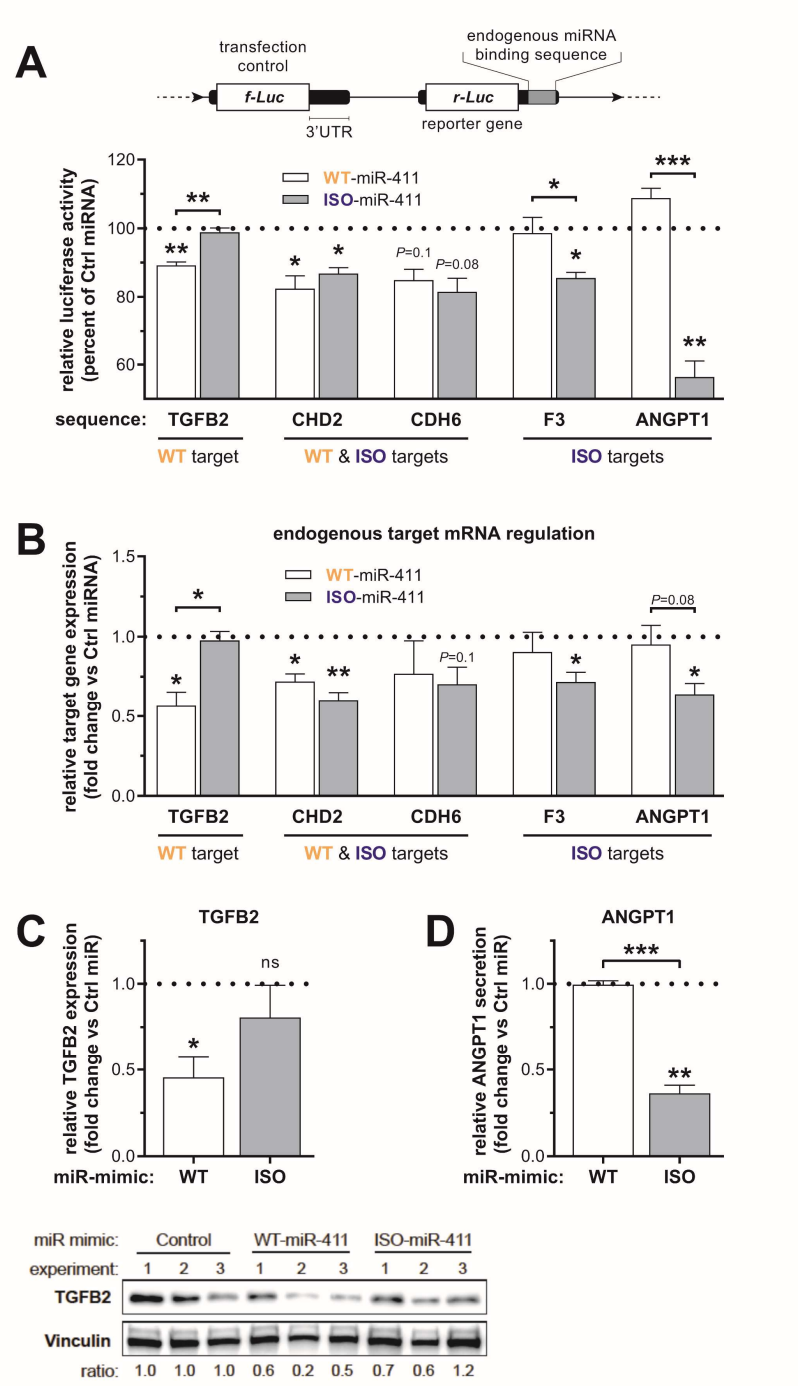

Figure 6: **Validation of differential target sequence binding and endogenous target regulation.** (A) Schematic representation of the luciferase constructs that were used to examine the binding of WT-miR-411 and ISO-miR-411 to endogenous miRNA binding sequences from selected putative target genes. The selected genes predicted targets of either WT-miR-411 or ISO-miR-411 or both as indicated. Constructs were co-transfected with either WT-miR-411, ISO-miR-411 or a non-targeting miRNA mimic (Ctrl miRNA) into HeLa cells. MicroRNA specific target site binding was assessed by examining luciferase reporter activity relative to that of the Ctrl miRNA (dotted line). (B) Endogenous target mRNA regulation relative to Ctrl miRNA treatment after transfection of HUAFs with microRNA mimics as indicated. (C) Relative TGFB2 protein expression in HUAF whole

◄ **Figure 6 continued**: cell lysates after transfection with indicated miRNA mimics as determined by Western blot. Expression was normalized per independent experiment to stable household protein Vinculin and expressed relative to Ctrl miRNA. (D) Relative ANGPT1 levels in the conditioned medium of transfected HUAFs. All data points represent normalized averages obtained from 3 independent experiments and are presented as mean ± SEM. **P*<0.05, ***P*<0.01, ****P*<0.001; by 1 sample *t* test versus Ctrl miRNA or 2-sided Student *t* test to compare WT-miRNA vs ED-miRNA treatments.

expression is regulated during processing from pre-miR-411 to mature miRNA, rather than during the biogenesis of the WT-pre-miR-411 and ISO-pre-miR-411. The seed sequence of ISO-miR-411 is shifted by 1 nucleotide compared to WT-miR-411. We demonstrate that this seed-sequence shift causes ISO-miR-411 to target a unique and larger set of mRNAs compared to WT-miR-411, leading to functional changes in the cellular response to ischemia.

We found that the expression of ISO-miR-411 compared to WT-miR-411 varies between tissues and that ISO-miR-411 expression is at least 3-fold higher than that of WT-miR-411 in human vascular cells and whole vascular tissue. These findings are

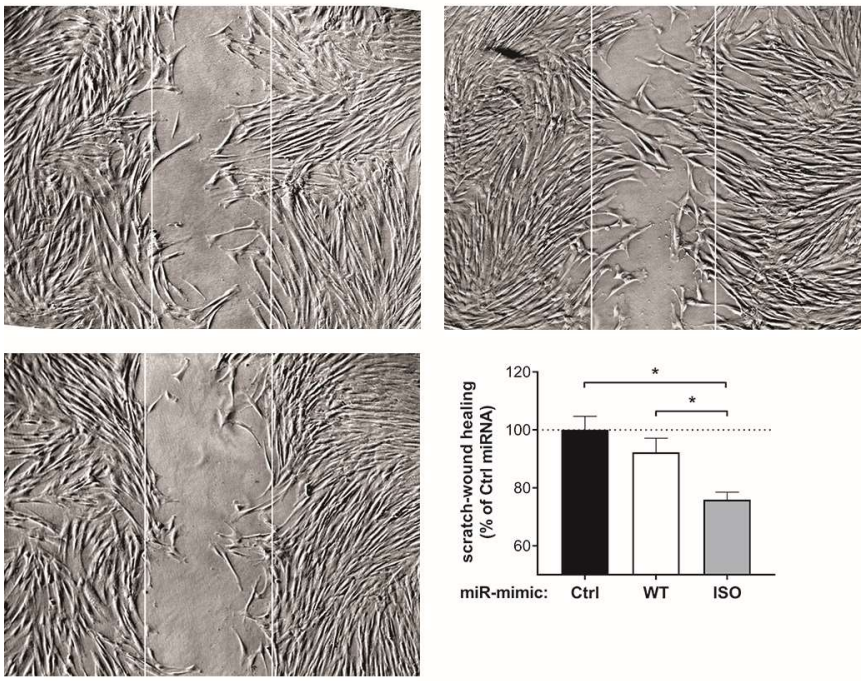

Figure 7: **The effect of WT-miR-411 and ISO-miR-411 on *in vitro* scratch-wound healing.** Representative images and quantification of HUAF scratch-wound healing after transfection with either WT-miR-411 (WT), ISO-miR-411 (ISO) or non-targeting miRNA mimic (Ctrl). White lines indicate original scratch wound area. Data points represent averages obtained from 3 independent experiments and are presented as mean ± SEM. **P*<0.05 by 2-sided Student *t* test.

consistent with previous studies which have shown that isomiRs in general can have tissue-specific expression.[21-23] The majority of these tissue-specific isomiRs were 3'-isomiRs however, which have an unaltered seed sequence. Nevertheless, a recent study showed that expression of a subset of 5'-isomiRs was tumor-specific enough to allow for tumor classification. Despite these findings, it remained unclear if changes in ISO/WT-miRNA ratio can be induced in response to pathophysiological changes. With the differential regulation of WT-miR-411 and ISO-miR-411 expression under ischemia, we provide evidence that 5'-isomiR expression can indeed respond to pathophysiological changes.

5'-isomiR are generally formed by cleavage variations of either DROSHA or DICER during miRNA biogenesis.[10,35] MiR-411 is located on the 5'-pri-microRNA arm, which means DROSHA cleavage introduces the 5'-end variation when cutting pri-miR-411 to pre-miR-411. We found abundant ISO-pre-miR-411 expression, which confirms that alternative DROSHA cleavage is responsible for the 5'-end variation of miR-411. The factors that influence alternative DROSHA cleavage are largely unknown. We hypothesized that DROSHA's different isoforms could be responsible for cleavage variation. However, isoform expression profiles suggested that this is unlikely since the transcript of one isoform clearly dominates total *DROSHA* expression in our primary human fibroblasts.

It is assumed that the rate of differential cleavage that introduces the 5'-end variation determines the isomiR's abundance.[36,37] We found that ISO/WT-pre-miR-411 ratio increased under acute ischemia while the mature ISO/WT-miR-411 ratio decreased significantly. These findings demonstrate that the differential regulation of WT-miR-411 and ISO-miR-411 under ischemia is not caused by changes in DROSHA cleavage. If not by DROSHA, changes in ISO/WT-miR-411 ratios can either be caused by changes in DICER substrate selection and cleavage or by altered microRNA turnover rates. Indeed, it has been shown that isomiRs of the same microRNA display different turnover rates. Although still poorly understood, a larger body of evidence indicates sequence variations in the 3'-end of the microRNA as responsible for altered turnover rates.[38] However, Guo et al showed for miR92b-3p, also a vasoactive microRNA, that isoforms with an adenosine added in front of the original uracil at the 5'-end, similar to ISO-miR-411, are less stable and cleared faster.[39] This was found in unchallenged

HDMYZ cells however, so it was not investigated whether ischemia would alter these clearance rates. Although we cannot exclude an effect of altered isomiR turnover under ischemia, we do provide evidence here that the altered ISO-miR-411/WT-miR-411 ratio is, at least in part, introduced during the final maturation step from pre-miR-411 to mature miR-411.

Several studies have shown that the ISO/WT-miRNA ratios of 5'-isomiRs generated by alternative DICER cleavage can be modulated by DICERs cofactors TRBP and PACT.[36,40] While we did observed a decrease in the expression of *TRBP* and *PACT* under ischemia, this is unlikely to be responsible for regulating the ISO/WT-miR-411 ratio since the DICER cleavage site is identical for both miR-411 variants. However, we observed an initial increase of miR-411 expression under ischemia, which coincided with increased *ADAR1* and *ADAR2* expression. ADAR1 facilitates microRNA biogenesis via direct interaction with DICER in order to increase its cleavage efficiency.[31,41,42] Therefore, we hypothesized that ADARs play a role in regulation of WT-miR-411 and ISO-miR-411. Even though ADARs did not affect ISO/WT-miR-411 ratio, we found that knockdown of ADAR1 decreased WT- and ISO-miR-411 expression. Simultaneously, expression of their pre-miRNAs increased, indicating that pre-miR-411 processing efficiency was decreased. These findings add to the growing body of evidence that ADAR1 regulates microRNA expression and function under pathological conditions.[30,32,42,43] Besides ADAR1, many other RNA binding proteins (RBPs) can impact the processing of microRNAs in a highly (sequence-) specific manner.[44] We have recently shown that the Cold Inducible RBP (CIRBP) and HADHB regulate processing of miR-329 and miR-495, but not of other closely related microRNAs under ischemia.[45] The Myocyte enhancer factor 2A (MEF2A), which is known as a DNA binding protein, also functions as an RBP, regulating microRNA biogenesis in a microRNA-specific manner.[46] A recent study by Treiber et al even showed that many, if not all, individual microRNAs have their own RBP to facilitate microRNA biogenesis.[47] Therefore, it is not at all unlikely that that there are also isomiR-specific RBPs that regulate their processing and expression.

We found that the ISO/WT-miR-411 ratio is decreased in response to acute ischemia, in cultured fibroblasts, but also in murine muscle tissue. ISO-miR-411 has a unique seed-sequence that is different from WT-miR-411 as well as from any other any

known microRNA.[33] We demonstrate that WT-miR-411 but not ISO-miR-411 downregulates TGFB2 expression, a cytokine that affects many cellular processes, including angiogenesis.[48,49] ISO-miR-411 on the other hand, specifically downregulates the expression of both F3 and ANGPTl, which can both stimulate cell migration and wound healing.[50-53] Consistent with these findings, our *in vitro* scratch-wound healing assays demonstrate that ISO-miR-411 treatment decreases cell migration and wound closure, whereas WT-miR-411 does not. These findings imply that ISO-miR-411 is downregulated in response to acute ischemia in order to allow for a pro-angiogenic response that is further facilitated by an increase in the pro-angiogenic WT-miR-411. In patients with end-stage PAD, the pro-angiogenic response is generally insufficient. We observed an increase in the ISO-miR-411/WT-miR-411 ratio in lower limb veins from end-stage PAD patients, which may contribute to the lack of efficient neovascularization in these patients.

In conclusion, we demonstrate that miR-411 has a 5'-isomiR that is abundantly expressed in the vasculature. Maturation of WT-pre-miR-411 and ISO-pre-miR-411 are differentially regulated in the response to acute ischemia, resulting in a decreased mature ISO/WT-miR-411 ratio, both *in vitro* and *in vivo*. ISO-miR-411 has a unique targetome, which includes the pro-angiogenic genes *F3* and *ANGPTl*. In contrast to WT-miR-411, ISO-miR-411 decreased *in vitro* scratch-wound healing, demonstrating that ISO-miR-411 and WT-miR-411 have distinct biological functions.

By showing that the formation of isomiRs is an actively regulated process and that isomiRs have individual sets of target genes that differ from that of the canonical microRNAs, we demonstrate, for the first time in a cardiovascular setting, that yet another level of active regulation of gene and protein expression exists within the emerging field of noncoding RNAs. At this point, the impact of the reported findings cannot yet be overseen, but we are convinced that isomiRs will prove to be of importance in future microRNA-based therapeutic strategies.

MATERIALS AND METHODS

MiR-411 expression in publicly available microRNA-seq datasets

Publicly available microRNA-seq datasets were analyzed to examine ISO-miR-411 versus WT-miR-411 expression in human and murine tissues.

For human tissues, the following datasets were analyzed using the 'miR-seq browser' function of the miRGator webtool (mirgator.kobic.re.kr)[54]: SRX050631 (heart), GSM548639 (whole brain), SRX050632 (lung), SRX050637 (kidney), SRX050638 (liver), GSM769005 (skin), SRX050635 (testes), SRX050634 (ovary), SRX050633 (thymus), SRX050636 (spleen), GSM494810 (PBMCs) and GSM1279746 (plasma).

For murine tissues, the following datasets were analyzed using the IsomiR Bank webtool (mcg.ustc.edu.cn/bsc/isomir)[55]: GSM539868 (heart), GSM539869 (brain), GSM539870 (lung), GSM539872 (kidney), GSM539871 (liver), GSM539874 (skin), GSM539877 (testicular), GSM539878 (ovaries), GSM539873 (pancreatic), GSM539876 (salivary gland), GSM510457-GSM510460 (day 12.5 embryos), GSM510461-GSM510464 (day 9.5 embryos), GSM510465-GSM510468 (day 7.5 embryos), GSM510445-GSM510456 (whole body newborn mice), GSM314552 & GSM314558 (Wild type ESCs), GSM314557 & GSM314559 (DGCR8 knock out ESCs) and GSM314553 (Dicer knock out ESCs).

In each case, we extracted the number of WT-miR-411 and ISO-miR-411 reads or reads per million within a particular sample. The ISO/WT-miR-411 ratio was simply calculated by dividing the ISO-miR-411 reads by the WT-miR-411 reads.

Isolation of primary vascular cells from human umbilical cords

Isolation and culturing of primary human umbilical arterial fibroblasts (HUAF) was performed as described previously[25,30].

In brief, umbilical cords were collected from full-term pregnancies and used for either human umbilical arterial fibroblasts (HUAF) or human umbilical venous endothelial cells (HUVEC) isolation.

For HUAF isolation, the tunica adventitia was removed from the umbilical artery and incubated overnight in serum rich medium (DMEM GlutaMAX™ (Invitrogen, GIBCO, Auckland, New Zealand), 10% heat inactivated fetal bovine serum (PAA, Pasching, Austria), 10% heat inactivated human serum, 100 U penicillin and 100 µg streptomycin per mL (Lonza, Basel, Switzerland) and nonessential amino acids (GIBCO #11140050)). The next day the adventitia was incubated in a 2mg/ml collagenase type II solution (Worthington, Lakewood, NJ, USA) at 37 °C. The resulting

cell suspension was filtered over a 70µm cell strainer, pelleted, resuspended and plated in HUAF culture medium (DMEM GlutaMAX™ (Invitrogen), 10% heat inactivated fetal bovine serum (PAA) and 100U penicillin and 100ug streptomycin per mL (Lonza)).

HUVECs were isolated from the umbilical veins by infusing a flushed vein with 0.75 mg/ml collagenase type II (Worthington) and incubated at 37°C for 20 minutes. The cell suspension was collected and pelleted and resuspended in HUVEC culture medium (M199 (PAA), 10% heat inactivated human serum (PAA), 10% heat inactivated newborn calf serum (PAA), 100 U penicillin and 100 µg streptomycin per mL (Lonza), 150µg/ml endothelial cell growth factor (kindly provided by Dr. Koolwijk, VU Medical Center, Amsterdam, The Netherlands) and 5 U/ml heparin (LEO Pharma, Ballerup, Denmark)). HUVECs were cultured in plates coated with 10 µg/ml fibronectin (Sigma-Aldrich, Steinheim, Germany).

Primary cell culture

Cells were cultured at 37°C in a humidified 5% CO_2 environment. Culture medium was refreshed every 2-3 days. Cells were passed using trypsin-EDTA (Sigma-Aldrich) at 70-80% confluency (HUAFs) or 90-100% (HUVECs). HUAFs were used up to passage five and HUVECs up to passage three. Stock solutions of isolated HUAFs and HUVECs up to passage two were stored at -180°C in DMEM GlutaMAX™ containing 20% FBS and 10% DMSO (Sigma-Aldrich).

In vitro ischemia model

For *in vitro* ischemia experiments, HUAFs were seeded in separate 12 well plates at 70.000 cells per well and subsequently cultured in either: control conditions for 48h (normal culture medium and ~20% oxygen), 48h ischemic conditions (starvation medium and hypoxia of 1% oxygen) or 24h ischemic conditions (initial 24h normal culture medium and ~20% oxygen followed by 24h starvation medium and hypoxia of 1% oxygen). Starvation medium consisted of DMEM GlutaMAX™ (Invitrogen) with 0.1% heat inactivated fetal bovine serum (PAA) and 100 U penicillin and 100 µg streptomycin per mL (Lonza). For consistency with the 24h ischemic conditions group, medium of the 48h control condition and 48h ischemic condition groups was also refreshed after 24h. At the end of the experiment, cells were washed with phosphate-buffered saline (PBS) and harvested with TRIzol Reagent (Invitrogen).

RNA isolation and cDNA synthesis

Total RNA was isolated with TRIzol (Invitrogen), according to the manufacturer's instructions. RNA concentration and purity were examined by nanodrop (Nanodrop Technologies, Wilmington, DE, USA). For pri-miRNA experiments, DNase treatment was performed using RQ1 RNase-Free DNase (Promega, Madison, WI, USA) according to manufacturer's instructions. Total complementary DNA (cDNA) was prepared using the High Capacity cDNA Reverse Transcription Kit (Applied Biosystems, Foster City, CA, USA) according to manufacturer's protocol.

Specific quantification of WT- and ISO-miR-411 by 5' Dumbbell-PCR

The expression of WT-miR-411 and ISO-miR-411 was quantified using a self-designed TaqMan qPCR assay specific enough to distinguish the one nucleotide difference at the 5'-end of the miRNAs. The assay was designed and performed based on the previously described 5'-DB-PCR method.[56,57] An overview of primer, probe and adapter sequences are provided in **Supplementary Table II**.

In brief, 50ng of total RNA were combined with 5pmol synthetic 5'-adapters (synthesized by Integrated DNA Technologies, IDT) which are specific for either WT-miR-411 or ISO-miR-411. After heating the samples to 90 °C for 3 min, the samples were buffered with Tris-HCl and $MgCl_2$ (Invitrogen) (final concentration 5 mM and 10 mM respectively, pH 8.0). The 5'-adapters were then annealed to the WT-miR-411 or ISO-miR-411 within the sample (20 min at 37 °C) and subsequently ligated to each other at 37°C for 30 min using T4 RNA Ligase 2 (Rnl2; New England Biolabs, Ipswich, MA, USA), followed by overnight incubation at 4°C. After reheating the samples to 90 °C for 2 min, reverse transcription of the ligated RNA was performed using the High Capacity cDNA Reverse Transcription Kit (Applied Biosystems) and a miR-411 specific RT primer (1 µM). The expression of WT-miR-411 and ISO-miR-411 within cDNA samples was quantified by qPCR using WT-miR-411 or ISO-miR-411 specific PrimeTime LNA probes combined with a primer set specific for the ligated RNA product. The specificity of the assay was confirmed using synthetic sequences (**Supplemental Figure I**). qPCRs were performed on the ViiA7 Real-Time PCR System (Applied Biosystems) using TaqMan Universal PCR Master Mix (Applied Biosystems). MiR-411 expression was normalized against noncoding household RNA *U6*, also quantified by a

TaqMan assay (Applied Biosystems). In all graphs, the expression of WT-miR-411 and ISO-miR-411 is presented as fold change, relative to the expression of WT-miR-411 in the control condition.

WT-pre-miR-411 and ISO-pre-miR-411 were quantified using the same 5'-DB-PCR method, but instead using pre-miR-411 specific primers.

Quantification of mRNA expression

The expression of mRNAs within cDNA samples was quantified by qPCR using Quantitect SYBR Green (QIAGEN) on the ViiA7 Real-Time PCR System (Applied Biosystems). mRNA expression was measured with intron-spanning primers and normalized against *RPLP0* mRNA expression, a household gene that remains stable under ischemic conditions[29]. All primer sequences are provided in **Supplementary Table III**.

siRNA mediated knockdown of ADAR1 and ADAR2

Knockdown of ADAR1 and ADAR2 in HUAFs was performed as previously described[30]. Briefly, HUAFs were seeded in 12 well plates, grown to 70% confluence and then transfected using Lipofectamine RNAiMAX (Invitrogen) according to the manufacturer's protocol, with a final concentration of 27.5 nM siRNA. siRNA sequences used were originally reported and validated by Stellos *et al.*[29] and can be found in **Supplemental Table VI**. After 48 hours, cells were washed 3 times with PBS and total RNA was isolated and cDNA was synthesized as before. Expression of *ADAR1*, *ADAR2* and *RPLP0* was quantified to determine knockdown efficiency. Subsequent microRNA expression analyses were performed as described above.

Hindlimb Ischemia Model

All animal experiments were approved by the committee on animal welfare of the Leiden University Medical Center (Leiden, The Netherlands, approval reference number 09163).

Adult male C57Bl/6 mice, 8 to 12 weeks old (Charles River, Wilmington, MA, USA) were housed in groups of 3 to 5 animals, with free access to tap water and regular chow. The assignment of the mice to the experimental groups was conducted randomly.

Induction of HLI was performed as described previously[30]. In brief, mice were anesthetized by intraperitoneal injection of midazolam (5mg/kg, Roche Diagnostics, Almere, The Netherlands), medetomidine (0.5mg/kg, Orion, Espoo, Finland) and fentanyl (0.05mg/kg, Janssen Pharmaceuticals, Beerse, Belgium). Unilateral HLI was induced by electrocoagulation of the left femoral artery proximal to the superficial epigastric arteries. After surgery, anesthesia was antagonized with flumazenil (0.5mg/kg, Fresenius Kabi, Bad Homburg vor der Höhe, Germany), atipamezole (2.5mg/kg, Orion) and buprenorphine (0.1mg/kg, MSD Animal Health, Boxmeer, The Netherlands). Mice were sacrificed by cervical dislocation and the adductor and gastrocnemius muscles were excised en bloc and snap-frozen on dry ice before (T0) and at 1 and 3 days (T1 and T3 respectively) after induction of HLI. Muscle tissues were crushed with pestle and mortar, while using liquid nitrogen to preserve sample integrity. Tissue homogenates were stored at -80°C. Total RNA was isolated from tissue powder by standard TRIzol-chloroform extraction as before.

Collection of human lower limb vein samples

Human lower limb vein (LLV) samples were collected at the Leiden University Medical Center.

Surplus LLV tissue from patients with CAD was collected during coronary bypass-surgery. These samples were anonymized and no data were recorded that could potentially trace back to an individual's identity. Collection, storage, and processing of the samples were performed in compliance with the Medical Treatment Contracts Act (WGBO, 1995) and the Code of Conduct for Health Research using Body Material (Good Practice Code, Dutch Federation of Biomedical Scientific Societies, 2002) and the Dutch Personal Data Protection Act (WBP, 2001).

Furthermore, LLVs from 8 patients with end-stage PAD were obtained directly after lower limb amputation. Inclusion criteria for the biobank were a minimum age of 18 years and lower limb amputation, excluding ankle, foot, or toe amputations. The exclusion criteria were suspected or confirmed malignancy and inability to give informed consent. Sample collection was approved by the Medical Ethics Committee of the Leiden University Medical Center (Protocol No. P12.265) and written informed consent was obtained from these participants.

All LLV samples were snap-frozen and stored at -80°C. Frozen LLV tissues were crushed in liquid nitrogen and total RNA was isolated from tissue powder by standard TRIzol-chloroform extraction as described above.

In silico target prediction and pathway enrichment analysis

Putative targetomes of WT-miR-411 and ISO-miR-411 were determined using three distinct target prediction algorithms to reduce the number of false positives: Targetscan (www.targetscan.org)[33], miRanda (www.microRNA.org)[58] and Diana-MR-microT (diana.imis.athena-innovation.gr)[59]. Targetscan (version 6.2) and miRanda (2010 release) predictions were obtained through the miRmut2go webtool (compbio.uthsc.edu/miR2GO)[60] whereas Diana-MR-microT predictions were obtained using its website. No restrictions were applied for target prediction. Genes were only considered to be a particular microRNA's putative target gene if each of the 3 target prediction algorithms identified them as a target.

For each targetome, the set of target genes of a particular microRNA, overrepresented pathways were identified using PANTHER pathway enrichment analysis (www.pantherdb.org, version 11)[34] as described previously.[61]

Dual Luciferase Reporter Gene Assays

Constructs: 3'UTR sequences containing one or more WT-miR-411 or ISO-miR-411 binding sites from endogenous target genes were amplified from HUAF cDNA using primers with a short extension containing cleavage sites for XhoI (5'-end) and NotI (3'-end) (**Supplemental Table III**). For *ANGPT1* the endogenous binding sequence was purchased from IDT (Integrated DNA Technologies, Coralville, USA) instead (**Supplemental Table IV**).

Amplicons and synthetic sequences were cloned in the PsiCHECK™-2 vector (Promega) at the 3'-end of the coding region of the Renilla luciferase reporter gene. The sequence of each construct was confirmed.

Sequences of the primers used are available in **Supplemental Table III**.

Luciferase Assays: HeLa cells were cultured at 37°C under 5% CO_2 using DMEM (GIBCO) with high glucose and stable L-glutamine, supplemented with 10% fetal calf serum and 100U penicillin and 100ug streptomycin per mL (Lonza). For experiments, HeLa cells were grown to 75-80% confluence in white 96 well plates. Lipofectamine

3000 (Invitrogen) in Opti-MEM (GIBCO) was used, according to manufacturer's instructions, to transfect each well with 30ng of PsiCHECK2-vector containing endogenous miRNA binding sequences or the original empty vector. Cells were co-transfected with 2 pmol miRcury LNA miRNA mimic for either a WT-miR-411, ISO-miR-411 or negative control miRNA (QIAGEN). Firefly- and Renilla-luciferase were measured in cell lysates using a Dual-Luciferase Reporter Assay System (Promega) according to manufacturer's protocol on a Cytation™ 5 plate reader (BioTek, Winooski, VT, USA). Firefly luciferase activity was used as an internal control for cellular density and transfection efficiency. The luminescence ratios were corrected for differences in baseline vector luminescence observed in vehicle treated group and expressed as percentage of scrambled control luminescence.

Displayed luciferase data represent the normalized averages from three independent experiments.

Endogenous transcript regulation by WT-miR-411 or ISO-miR-411

Endogenous transcript regulation was examined by overexpression of WT-miR-411 or ISO-miR-411 in HUAFs. HUAFs were seeded in 12 wells plates at 70.000 cells per well and grown for 12h in culture medium after which the medium was replaced with starvation medium to synchronize cell cycle. After another 12h, Lipofectamine RNAiMAX (Invitrogen) in Opti-MEM (GIBCO) was used according to manufacturer's instructions to transfect each well with 0.1pg of miRcury LNA miRNA mimic for either a WT-miR-411, ISO-miR-411 or negative control miRNA (QIAGEN). After 12h, transfection medium was replaced with new starvation medium. After 14h (26h total after transfection), cells were washed twice with PBS and harvested with TRIzol reagent, after which RNA was isolated, total cDNA was prepared and target mRNA expression was measured by qPCR as described above. Target mRNA expression was normalized against *RPLP0*. The intron spanning primers used can be found in **Supplemental Table III**. Displayed endogenous target regulation represent the normalized averages from three independent experiments.

Regulation of TGFB2 and ANGPT1 by WT-miR-411 or ISO-miR-411

Endogenous protein regulation was also examined by overexpression of WT-miR-411 or ISO-miR-411 in HUAFs through transfection. This time, 50.000 cells per well

were seeded per well in 12 wells plates to grow for 12h in culture medium followed by synchronization by switching to starvation medium for 6h. HUAFs were then transfected with 0.1pg of miRcury LNA miRNA mimic for either a WT-miR-411, ISO-miR-411 or negative control miRNA (QIAGEN), using Opti-MEM (GIBCO) and Lipofectamine RNAiMAX (Invitrogen) according to manufacturer's instructions. 48h after transfection, conditioned medium was collected, cells were washed twice with PBS and harvested with TRIzol reagent (Invitrogen).

No TGFB2 could be detected in the HUAF conditioned medium using the Human TGF-beta 2 Quantikine ELISA Kit (DB250, R&D systems, Minneapolis, MN, USA) according to manufactures instructions. Therefore, protein was isolated from cell lysates with TRIzol (Invitrogen), according to the manufacturer's instructions. Total protein concentration was quantified by Pierce BCA Protein Assay Kit (ThermoFisher Scientific) after which protein concentration was normalized to 1µg/µL in Laemmli buffer (Bio-Rad Laboratories, Hercules, CA, USA) containing 10% β-mercaptoethanol (Sigma-Aldrich).

Samples were heated to 95°C for 5 minutes and cooled before loading 1 µg of protein per lane in a 4–15% Mini-PROTEAN TGM Precast Protein Gel (Bio-Rad Laboratories). Protein separation was performed in Vertical Electrophoresis Cell using premixed Tris/glycine/SDS running buffer (both Bio-Rad Laboratories). Proteins were transferred onto a nitrocellulose membrane (GE Healthcare Life Sciences, Eindhoven, The Netherlands) by a wet transfer using premixed Tris/glycine transfer buffer (Bio-Rad Laboratories). The membrane was blocked at room temperature in 5% non-fat dried milk in TBS-T (150mM NaCl; 50mM Tris; 0,05% Tween-20 (Sigma-Aldrich)) and subsequently incubated overnight at 4ºC with antibodies for TGFB2 (ab36495, Abcam, Cambridge, UK) or stable household protein Vinculin (hVIN-1, Novus Biologicals, Centennial, CO, USA), diluted to 1:500 in 5% non-fat dried milk in TBS-T. After multiples washes with TBS-T, the membrane was incubated at room temperature with anti-mouse peroxidase conjugated secondary antibody (31432, ThermoFisher Scientific), diluted to 1:10000 in 5% non-fat dried milk in TBS-T. Proteins of interest were revealed using SuperSignal™ West Pico PLUS Chemiluminescent Substrate (ThermoFisher Scientific) and imaged using the ChemiDoc Touch Imaging System

(Bio-Rad Laboratories). TGFB2 expression was quantified relative to stable household protein Vinculin using ImageJ.

Levels of secreted ANGPT1 in HUAF conditioned medium were quantified using the Human Angiopoietin-1 Quantikine ELISA Kit (DANG10, R&D systems, Minneapolis, MN, USA) according to manufactures instructions.

Displayed endogenous protein regulation represent the normalized averages from three independent experiments.

Scratch-wound healing assays

Effects of WT-miR-411 or ISO-miR-411 overexpression on scratch-wound healing of HUAFs were examined. HUAFs were seeded and transfected as described above. Transfection medium was removed after 12h. Next, a p200 pipette tip was used to introduce a scratch-wound across the diameter of each well. Subsequently, the cells were washed with sterile PBS and medium was replaced with new serum starvation medium. Three locations along the scratch-wound were marked per well. The scratch-wound at these sites was imaged at time 0h and 14h after scratch-wound introduction using live phase-contrast microscopy (Axiovert 40C, Carl Zeiss, Oberkochen, Germany). After the 14h timepoint, cells were washed 3 times in PBS and then lysed and harvested in TRIzol for RNA isolation as before. MiRNA overexpression efficiency was validated by measuring miRNA expression as described above. For each imaged location, the area of the scratch-wound at 0h was superimposed on the 14h scratch-wound area image. Scratch-wound healing was then determined per well as the newly covered scratch-wound area after 14h using the wound healing tool macro for ImageJ. Displayed scratch-wound healing represent the averages from three independent experiments.

Statistical Analysis

All results are expressed as mean ± SEM. Since all variables measured were continuous parameters, pairwise comparisons were tested using *t*-tests. *P*-values less than or equal to 0.05 were considered statistically significant.

ACKNOWLEDGEMENTS

We thank M.R. de Vries for obtaining the HLI samples and E.A.C. Goossens, K.H. Simons and the vascular and thoracic surgeons of the LUMC who collected the patient material.

Author Contributions

Conceptualization – AYN and PHAQ; Methodology – RVCTK and AYN; Investigation – RVCTK and TW; Writing – Original Draft – RVCTK; Writing – Review & Editing – RVCTK, TW, PHAQ and AYN; Funding Acquisition – AYN; Supervision – PHAQ and AYN.

Sources of funding

This study was supported by a grant from the Dutch Heart Foundation (Dr. E. Dekker Senior Postdoc, 2014T102), the LUMC Johanna Zaaijer Fund (2017) and the Austrian Science Fund FWF (Lise Meitner Grant, M 2578-B30).

Disclosures

None.

REFERENCES

1. Hellingman AA, Bastiaansen AJ, de Vries MR, Seghers L, Lijkwan MA, Lowik CW, Hamming JF, Quax PH. Variations in surgical procedures for hind limb ischaemia mouse models result in differences in collateral formation. *European journal of vascular and endovascular surgery : the official journal of the European Society for Vascular Surgery*. 2010;40:796-803
2. Bartel DP. MicroRNAs: genomics, biogenesis, mechanism, and function. *Cell*. 2004;116:281-297
3. Zhao Y, Ransom JF, Li A, Vedantham V, von Drehle M, Muth AN, Tsuchihashi T, McManus MT, Schwartz RJ, Srivastava D. Dysregulation of cardiogenesis, cardiac conduction, and cell cycle in mice lacking miRNA-1-2. *Cell*. 2007;129:303-317
4. Weber C. MicroRNAs: from basic mechanisms to clinical application in cardiovascular medicine. *Arteriosclerosis, thrombosis, and vascular biology*. 2013;33:168-169
5. Welten SM, Goossens EA, Quax PH, Nossent AY. The multifactorial nature of microRNAs in vascular remodelling. *Cardiovascular research*. 2016;110:6-22
6. Friedman RC, Farh KK, Burge CB, Bartel DP. Most mammalian mRNAs are conserved targets of microRNAs. *Genome Res*. 2009;19:92-105
7. Brennecke J, Stark A, Russell RB, Cohen SM. Principles of microRNA-target recognition. *PLoS Biol*. 2005;3:e85
8. Lewis BP, Shih IH, Jones-Rhoades MW, Bartel DP, Burge CB. Prediction of mammalian microRNA targets. *Cell*. 2003;115:787-798
9. Han J, Lee Y, Yeom KH, Nam JW, Heo I, Rhee JK, Sohn SY, Cho Y, Zhang BT, Kim VN. Molecular basis for the recognition of primary microRNAs by the Drosha-DGCR8 complex. *Cell*. 2006;125:887-901
10. Neilsen CT, Goodall GJ, Bracken CP. IsomiRs--the overlooked repertoire in the dynamic microRNAome. *Trends Genet*. 2012;28:544-549
11. Lee Y, Ahn C, Han J, Choi H, Kim J, Yim J, Lee J, Provost P, Radmark O, Kim S, Kim VN. The nuclear RNase III Drosha initiates microRNA processing. *Nature*. 2003;425:415-419
12. Ha M, Kim VN. Regulation of microRNA biogenesis. *Nat Rev Mol Cell Biol*. 2014;15:509-524
13. Kobayashi H, Tomari Y. RISC assembly: Coordination between small RNAs and Argonaute proteins. *Biochimica et biophysica acta*. 2016;1859:71-81
14. Kozomara A, Birgaoanu M, Griffiths-Jones S. miRBase: from microRNA sequences to function. *Nucleic Acids Res*. 2019;47:D155-d162
15. Landgraf P, Rusu M, Sheridan R, et al. A mammalian microRNA expression atlas based on small RNA library sequencing. *Cell*. 2007;129:1401-1414
16. Kuchenbauer F, Morin RD, Argiropoulos B, et al. In-depth characterization of the microRNA transcriptome in a leukemia progression model. *Genome Res*. 2008;18:1787-1797
17. Starega-Roslan J, Krol J, Koscianska E, Kozlowski P, Szlachcic WJ, Sobczak K, Krzyzosiak WJ. Structural basis of microRNA length variety. *Nucleic Acids Res*. 2011;39:257-268
18. Wu H, Ye C, Ramirez D, Manjunath N. Alternative processing of primary microRNA transcripts by Drosha generates 5' end variation of mature microRNA. *PLoS One*. 2009;4:e7566
19. Cloonan N, Wani S, Xu Q, et al. MicroRNAs and their isomiRs function cooperatively to target common biological pathways. *Genome Biol*. 2011;12:R126
20. Llorens F, Banez-Coronel M, Pantano L, del Rio JA, Ferrer I, Estivill X, Marti E. A highly expressed miR-101 isomiR is a functional silencing small RNA. *BMC Genomics*. 2013;14:104

21. Loher P, Londin ER, Rigoutsos I. IsomiR expression profiles in human lymphoblastoid cell lines exhibit population and gender dependencies. *Oncotarget*. 2014;5:8790-8802
22. Telonis AG, Loher P, Jing Y, Londin E, Rigoutsos I. Beyond the one-locus-one-miRNA paradigm: microRNA isoforms enable deeper insights into breast cancer heterogeneity. *Nucleic Acids Res*. 2015;43:9158-9175
23. Telonis AG, Magee R, Loher P, Chervoneva I, Londin E, Rigoutsos I. Knowledge about the presence or absence of miRNA isoforms (isomiRs) can successfully discriminate amongst 32 TCGA cancer types. *Nucleic Acids Res*. 2017;45:2973-2985
24. Small EM, Olson EN. Pervasive roles of microRNAs in cardiovascular biology. *Nature*. 2011;469:336-342
25. Welten SM, Bastiaansen AJ, de Jong RC, de Vries MR, Peters EA, Boonstra MC, Sheikh SP, La Monica N, Kandimalla ER, Quax PH, Nossent AY. Inhibition of 14q32 MicroRNAs miR-329, miR-487b, miR-494, and miR-495 increases neovascularization and blood flow recovery after ischemia. *Circ Res*. 2014;115:696-708
26. Muiwo P, Pandey P, Ahmad HM, Ramachandran SS, Bhattacharya A. IsomiR processing during differentiation of myelogenous leukemic cell line K562 by phorbol ester PMA. *Gene*. 2018;641:172-179
27. Bandara V, Michael MZ, Gleadle JM. Hypoxia represses microRNA biogenesis proteins in breast cancer cells. *BMC Cancer*. 2014;14:533
28. Bandara KV, Michael MZ, Gleadle JM. MicroRNA Biogenesis in Hypoxia. *Microrna*. 2017;6:80-96
29. Stellos K, Gatsiou A, Stamatelopoulos K, et al. Adenosine-to-inosine RNA editing controls cathepsin S expression in atherosclerosis by enabling HuR-mediated post-transcriptional regulation. *Nat Med*. 2016;22:1140-1150
30. van der Kwast RVCT, van Ingen E, Parma L, Peters HAB, Quax PHA, Nossent AY. Adenosine-to-Inosine Editing of MicroRNA-487b Alters Target Gene Selection After Ischemia and Promotes Neovascularization. *Circ Res*. 2018;122:444-456
31. Nishikura K, Sakurai M, Ariyoshi K, Ota H. Antagonistic and stimulative roles of ADAR1 in RNA silencing. *RNA Biol*. 2013;10:1240-1247
32. Nishikura K. A-to-I editing of coding and non-coding RNAs by ADARs. *Nat Rev Mol Cell Biol*. 2016;17:83-96
33. Agarwal V, Bell GW, Nam JW, Bartel DP. Predicting effective microRNA target sites in mammalian mRNAs. *eLife*. 2015;4
34. Mi H, Huang X, Muruganujan A, Tang H, Mills C, Kang D, Thomas PD. PANTHER version 11: expanded annotation data from Gene Ontology and Reactome pathways, and data analysis tool enhancements. *Nucleic Acids Res*. 2017;45:D183-D189
35. Bofill-De Ros X, Yang A, Gu S. IsomiRs: Expanding the miRNA repression toolbox beyond the seed. *Biochim Biophys Acta Gene Regul Mech*. 2019
36. Fukunaga R, Han BW, Hung JH, Xu J, Weng Z, Zamore PD. Dicer partner proteins tune the length of mature miRNAs in flies and mammals. *Cell*. 2012;151:533-546
37. Ma H, Wu Y, Choi JG, Wu H. Lower and upper stem-single-stranded RNA junctions together determine the Drosha cleavage site. *Proc Natl Acad Sci U S A*. 2013;110:20687-20692
38. Gebert LFR, MacRae IJ. Regulation of microRNA function in animals. *Nature Reviews Molecular Cell Biology*. 2019;20:21-37
39. Guo YW, Liu J, Elfenbein SJ, Ma YH, Zhong M, Qiu CH, Ding Y, Lu J. Characterization of the mammalian miRNA turnover landscape. *Nucleic Acids Research*. 2015;43:2326-2341
40. Kim Y, Yeo J, Lee JH, Cho J, Seo D, Kim JS, Kim VN. Deletion of human tarbp2 reveals cellular microRNA targets and cell-cycle function of TRBP. *Cell Rep*. 2014;9:1061-1074
41. Ota H, Sakurai M, Gupta R, Valente L, Wulff BE, Ariyoshi K, Iizasa H, Davuluri RV, Nishikura K. ADAR1 forms a complex with Dicer to promote microRNA processing and RNA-induced gene silencing. *Cell*. 2013;153:575-589

42. Heale BSE, Keegan LP, McGurk L, Michlewski G, Brindle J, Stanton CM, Caceres JF, O'Connell MA. Editing independent effects of ADARs on the miRNA/siRNA pathways. *Embo Journal*. 2009;28:3145-3156
43. Cho CJ, Myung SJ, Chang S. ADAR1 and MicroRNA; A Hidden Crosstalk in Cancer. *International journal of molecular sciences*. 2017;18
44. Michlewski G, Caceres JF. Post-transcriptional control of miRNA biogenesis. *Rna*. 2019;25:1-16
45. Velasco ADR, Welten SMJ, Goossens EAC, Quax PHA, Rappsilber J, Michlewski G, Nossent AY. Posttranscriptional Regulation of 14q32 MicroRNAs by the CIRBP and HADHB during Vascular Regeneration after Ischemia. *Mol Ther-Nucl Acids*. 2019;14:329-338
46. Welten SMJ, de Vries MR, Peters EAB, Agrawal S, Quax PHA, Nossent AY. Inhibition of Mef2a Enhances Neovascularization via Post-transcriptional Regulation of 14q32 MicroRNAs miR-329 and miR-494. *Mol Ther-Nucl Acids*. 2017;7:61-70
47. Treiber T, Treiber N, Plessmann U, Harlander S, Daiss JL, Eichner N, Lehmann G, Schall K, Urlaub H, Meister G. A Compendium of RNA-Binding Proteins that Regulate MicroRNA Biogenesis. *Molecular Cell*. 2017;66:270-+
48. Hofer E, Schweighofer B. Signal transduction induced in endothelial cells by growth factor receptors involved in angiogenesis. *Thromb Haemost*. 2007;97:355-363
49. Li C, Guo B, Bernabeu C, Kumar S. Angiogenesis in breast cancer: the role of transforming growth factor beta and CD105. *Microsc Res Tech*. 2001;52:437-449
50. Chen J, Kasper M, Heck T, et al. Tissue factor as a link between wounding and tissue repair. *Diabetes*. 2005;54:2143-2154
51. Xu Z, Xu H, Ploplis VA, Castellino FJ. Factor VII deficiency impairs cutaneous wound healing in mice. *Mol Med*. 2010;16:167-176
52. Koh GY. Orchestral actions of angiopoietin-1 in vascular regeneration. *Trends Mol Med*. 2013;19:31-39
53. Novotny NM, Lahm T, Markel TA, Crisostomo PR, Wang M, Wang Y, Tan J, Meldrum DR. Angiopoietin-1 in the treatment of ischemia and sepsis. *Shock (Augusta, Ga.)*. 2009;31:335-341
54. Cho S, Jang I, Jun Y, Yoon S, Ko M, Kwon Y, Choi I, Chang H, Ryu D, Lee B, Kim VN, Kim W, Lee S. MiRGator v3.0: a microRNA portal for deep sequencing, expression profiling and mRNA targeting. *Nucleic Acids Res*. 2013;41:D252-257
55. Zhang Y, Zang Q, Xu B, Zheng W, Ban R, Zhang H, Yang Y, Hao Q, Iqbal F, Li A, Shi Q. IsomiR Bank: a research resource for tracking IsomiRs. *Bioinformatics (Oxford, England)*. 2016;32:2069-2071
56. Shigematsu M, Honda S, Kirino Y. Dumbbell-PCR for Discriminative Quantification of a Small RNA Variant. *Methods Mol Biol*. 2018;1680:65-73
57. Honda S, Kirino Y. Dumbbell-PCR: a method to quantify specific small RNA variants with a single nucleotide resolution at terminal sequences. *Nucleic Acids Res*. 2015;43:e77
58. Betel D, Koppal A, Agius P, Sander C, Leslie C. Comprehensive modeling of microRNA targets predicts functional non-conserved and non-canonical sites. *Genome Biol*. 2010;11:R90
59. Paraskevopoulou MD, Georgakilas G, Kostoulas N, Vlachos IS, Vergoulis T, Reczko M, Filippidis C, Dalamagas T, Hatzigeorgiou AG. DIANA-microT web server v5.0: service integration into miRNA functional analysis workflows. *Nucleic Acids Res*. 2013;41:W169-173
60. Bhattacharya A, Cui Y. miR2GO: comparative functional analysis for microRNAs. *Bioinformatics (Oxford, England)*. 2015;31:2403-2405
61. Mi H, Muruganujan A, Casagrande JT, Thomas PD. Large-scale gene function analysis with the PANTHER classification system. *Nat Protoc*. 2013;8:1551-1566

CHAPTER 3

Supplemental Materials

Supplemental Figures

I. Specificity of WT-miR-411 and ISO-miR-411 quantification by Dumbbell-PCR
II. *In vitro* ischemia conditions induce HIF1A, VEGFA, SDF1 and p53.
III. Knockdown of ADAR1 and ADAR2 in primary vascular fibroblasts.
IV. Regulation of ISO/WT-411 ratio after overexpression of either WT-miR-411 or ISO-miR-411.

Supplemental Tables

I. Enriched pathways within WT-miR-411 and ISO-miR-411 targetomes
II. Sequences of WT-miR-411 and ISO-miR-411 specific Dumbbell-PCR
III. Primer sequences and purpose
IV. Sequences of siRNA and synthesized endogenous 3'UTRs

Supplemental References

SUPPLEMENTAL FIGURES

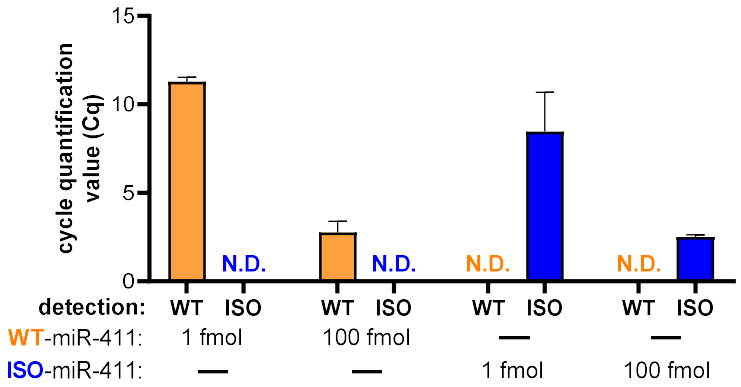

Supplemental Figure I: Specificity of WT-miR-411 and ISO-miR-411 quantification by Dumbbell-PCR. To quantify WT-miR-411 and ISO-miR-411 we designed TaqMan qPCR assay based on the previously described 5'-Dumbbell-PCR method.[1,2] The specificity of the assay was validated by performing quantification on synthetic sequences of either WT-miR-411 or ISO-miR-411 (n=3). When a signal was detected for either WT-miR-411 or ISO-miR-411, the resulting cycle quantification values are presented as mean ±SEM. When no signal was detected this is indicated as Not Detected (ND).

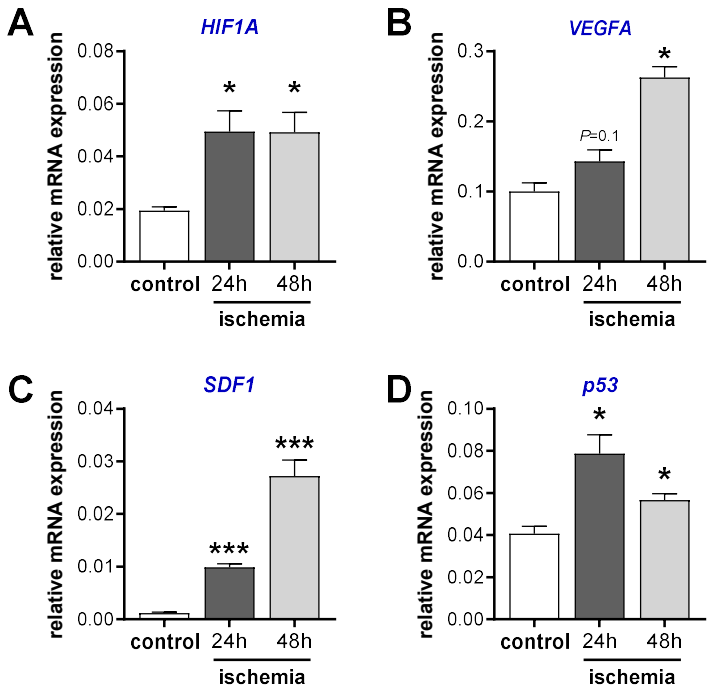

Supplemental Figure II: *In vitro* ischemia conditions induce HIF1A, VEGFA, SDF1 and p53. Primary human umbilical arterial fibroblasts (HUAFs) were cultured under normal or ischemic culture conditions, mimicked using a combination of hypoxia and serum starvation. Expression of hypoxia-inducible genes HIF1A (A), VEGFA (B), SDF1 (C) and cell cycle arrest marker p53 (D) were successfully increased upon ischemic culture conditions. All data are presented as mean ±SEM (n=3). **P*<0.05, ****P*<0.001; versus control condition unless otherwise indicated by 2-sided Student *t* test.

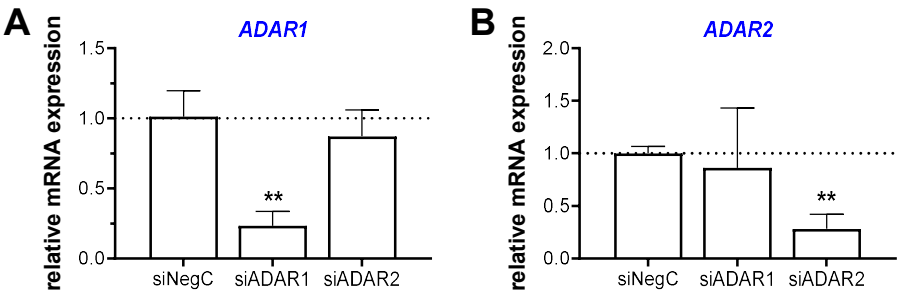

Supplemental Figure III: Knockdown of ADAR1 and ADAR2 in primary vascular fibroblasts. After transfecting HUAFs with a negative control, *ADAR1*-targeted or *ADAR2*-targeted siRNA (siNegC, siADAR1 and siADAR2 respectively), relative expression of *ADAR1* (A) and *ADAR2* (B) was measured by qRT-PCR to validate the knockdown efficiency and specificity. Data was expressed as fold change relative to siNegC and presented as mean ±SEM (n=3 per treatment).

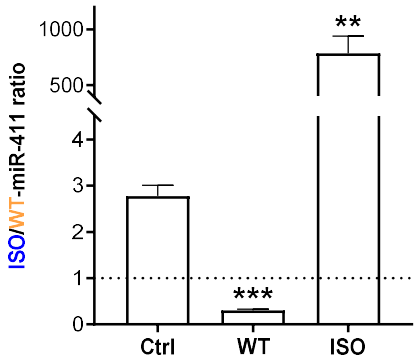

Supplemental Figure IV: Regulation of ISO/WT-411 ratio after overexpression of either WT-miR-411 or ISO-miR-411. HUAF samples were transfected with 0.1 pg of either a WT-miR-411 mimic (WT), an ISO-miR-411 mimic (ISO) or a control miRNA mimic (Ctrl). ISO/WT-miR-411 ratio was determined by 5'-DB-PCR. Overexpression of WT-miR-411 successfully reduced ISO/WT-miR-411 ratio compared to Ctrl and overexpression of ISO-miR-411 successfully increased ISO/WT-miR-411 ratio. Data are presented as mean ± SEM (n=3). ***P*<0.01, ****P*<0.001 versus Ctrl mimic by 2-sided Student *t* test.

SUPPLEMENTAL TABLES

Supplemental Table I. Enriched pathways within WT-miR-411 and ISO-miR-411 targetomes*

	Total genes mapped to pathway	# of mapped genes in target set	Expected # of genes targeted	Fold Enrichment	*P* value
WT-miR-411					
Cadherin signalling pathway	158	23	4.94	4.66	0.0000
Wnt signalling pathway	312	31	9.76	3.18	0.0000
shared targets of WT- and ISO-miR-411					
Cadherin signalling pathway	158	18	2.06	8.72	0.0000
Wnt signalling pathway	312	21	4.08	5.15	0.0000
ISO-miR-411					
Cadherin signalling pathway	158	24	9.69	2.48	0.0251
Wnt signalling pathway	312	38	19.13	1.99	0.0149

* Putative targetomes were analyzed by the PANTHER pathway algorithm[3]. Only pathway enrichments with $P<0.05$ after Bonferroni correction are reported.

Supplemental Table II. Sequences of WT-miR-411 and ISO-miR-411 specific Dumbbell-PCR

Component	Sequence
WT-miR-411	
5'-adapter	TCTACTACTCAGTGCGTGGGAGGGTGTGTGGTCTTGCTTGGTGTG CACTGrArG
miR-411 RT primer	TTCGTACGCTATAC
miR-411 qPCR primers	**F:** GAGGGTGTGTGGTCTTG **R:** TTCGTACGCTATACGGTC
pre-miR-411 RT primer	ACATACGTCACAGATAAAGCGT
pre-miR-411 qPCR primers	**F:** ACATACGTCACAGATAAAGCGT **R:** GAGGGTGTGTGGTCTTGCTT
TaqMan LNA probe	/Flu/CA**+C+T+G**A**+G+T+A**GT/3IABkFQ/
ISO-miR-411	
5'-adapter	CTACTATCTCAGTGCGTGGGAGGGTGTGTGGTCTTGCTTGGTGTG CACTGrArG
miR-411 RT primer	TTCGTACGCTATAC
miR-411 qPCR primers	**F:** GAGGGTGTGTGGTCTTG **R:** TTCGTACGCTATACGGTC
pre-miR-411 RT primer	ACATACGTCACAGATAAAGCGT
pre-miR-411 qPCR primers	**F:** ACATACGTCACAGATAAAGCGT **R:** GAGGGTGTGTGGTCTTGCTT
TaqMan LNA probe	/Flu/CAC**+T+G**A**+G+A+T+A**GT/3IABkFQ/

/Flu/, fluorophore; /3IABkFQ/, 3' Iowa Black® Fluorescence Quencher
Nucleotides in bold and preceded by a '+' are locked nucleic acid (LNA) nucleotides

Supplemental Table III: Primer sequences and purpose

Primer	Used for:	Sequence (5' to 3')
ADAR1_F	qPCR	GCTTGGGAACAGGGAATCGC
ADAR1_R		CGCAGTCTGGGAGTTGTATTTC
ADAR2_F	qPCR	GGAAGCTGCCTTGGGATCAG
ADAR2_R		GCTGCTGGAACTCATGTTTTCTTC
ANGPT1_F	qPCR	CCAGTACAACACAAACGCTCTG
ANGPT1-R		CTGCTGTATCTGGGCCATCTC
CDH2_F	qPCR	ATGCAAGACTGGATTTCCTGAAG
CDH2_R		TCTCACGGCATACACCATGC
CDH6_F	qPCR	GCTCTGGTTGCCATCCTTCTG
CDH6_R		CCACCTTCGTCGTTGTAACTG
DICER1_F	qPCR	ATCGCCTTCACTGCCTTTTG
DICER1_R		TTTTCAGCTAAAATCCGCAGG
DROSHA2_F	qPCR	AAAAAAGAGTATAAGAGATCTGGAAGGAG
DROSHA_R		CTCGGGCTCTTTTTCCTTG
DROSHA1_F	qPCR	AAAAAGAGTATAAGAGATCTGGAAGTCG
DROSHA_R		CTCGGGCTCTTTTTCCTTG
DROSHA3_F	qPCR	TACGAACGGAGCAGTCGC
DROSHA_R		CTCGGGCTCTTTTTCCTTG
DROSHA4_F	qPCR	GCTACGAACGGAGCAGGAG
DROSHA_ R		CTCGGGCTCTTTTTCCTTG
F3_F	qPCR	CAGCCCGGTAGAGTGTATGG
F3_R		GTGGGGAGTTCTCCTTCCAG
HIF1A_F	qPCR	TGTCTCTAGCCCTAGCTTGGTT
HIF1A_R		AGCAATATACCTGTGGCTGTCA
p53_F	qPCR	TGACACGCTTCCCTGGATTG
p53_R		TTTTCAGGAAGTAGTTTCCATAGGT
PACT_F	qPCR	CGTTGGTGACATAACCTGCAC
PACT_R		AGGCATTAAGGGGTCAGGAAC
RPLP0_F	qPCR	TCCTCGTGGAAGTGACATCG
RPLP0_R		TGTCTGCTCCCACAATGAAAC
TGFB2_F	qPCR	CCCTGCTGCACTTTTGTACC
TGFB2_R		AGGAGATGTGGGGTCTTCCC
TRBP_F	qPCR	CCTAATTTCACCTTCCGGGTCA
TRBP_R		GCAGTGAAGAGTCTAGGGGAGA
U6_F	qPCR	AGAAGATTAGCATGGCCCCT
U6_R		ATTTTGCGTGTCATCCTTGCG
VEGFa_F	qPCR	ATCACCATGCAGATTATGCGG
VEGFa_R		CCCCTTTCCCTTTCCTCGAAC
CDH2_3'UTR_F	Construct cloning	CTCTCTCGAGAGGGTGAACTTGGTTTTTGGAC
CDH2_3'UTR_R		CTGCGGCCGCACTTACTGCTCCCACCACAA
CDH6_3'UTR_F	Construct cloning	CTCTCTCGAGTCTAAAAAGTCATGATTCCCCCACT
CDH6_3'UTR_R		CTGCGGCCGCCGGCTCTGTTGGGCTAACG
F3_3'UTR_F	Construct cloning	CTCTCTCGAGTGGAAGGAAATTGGGTGCAT
F3_3'UTR_R		CTGCGGCCGCAGTCACCAAAATGTATTATAAGCG
TGFB2_3'UTR_F	Construct cloning	CTCTCTCGAGTTTGCCACATCATTGCAGAAG
TGFB2_3'UTR_R		CTGCGGCCGCCCTATCTGAGAGGAAAATGTCTGC

Gray highlighted sequences are primer extensions to flank the amplicon restriction enzyme sites

Supplemental Table IV: Sequences of siRNA and synthesized endogenous 3'UTRs

siRNA	targets	sequence
siADAR1	ADAR1	5'-GCUAUUUGCUGUCGUGUCA(dT)(dT)-3'
siADAR2	ADAR2	5'-GAUCGUGGCCUUGCAUUAA(dT)(dT)-3'
siRNA control:	nothing	5'-UCUCUCACAACGGGCAU(dT)(dT)-3'

3'UTR	sequence
ANGPT1 (ISO-miR-411 binding sites)	CTCTCTCGAGCTCGACTATAGAAAACTCCACTGACTGTCGGGCTTTAAAAAGGGAAGAAACTGCTGAGCT TGCTGTGCTTCAAA**CTACTA**CTGGACCTTATTTTGGAACTATGGTAGCCAGATGATAAATATGGTTAATT TCATGTAAAACAGAAAAAAAGAGTGAAAAAGAGAATATACATGAAGAATAGAAACAAGCCTGCCATAATC CTTTGGAAAAGATGTATTATACCAGTGAAAAGGTGTTATATCTATGCAAAC**CTACTA**ACAAATTATACTG TTGCACAATTTTGATAAAAATTTAGAACAGCATTGTCCTCTGAGTACATAGCATGTTTATATCTGCAAAA AACCTAATAGCTAATTAATCTGGAATATGCAACATTGTCCTTAATTGATGCAAATAACACAAATGCTCAA AGAAA**TCTACTAT**ATCCCTTAATGAAATACATCATTCTTCATATATTTCTCCTTCAGTCCATTCCCTTAG GCAATTTTTAATTTTTAAAAATTATTATCAGGGGAGAAAAATTGGCAAAACTATTATATGTAAGGGAAAT ATATACAAAAAGAAAATTAATCATAGTCACGCGGCCGCAG

Gray highlighted sequences are non-endogenous extensions containing restriction enzyme sites for cloning. Bold highlights indicate putative miRNA binding sites.

SUPPLEMENTAL REFERENCES

1. Shigematsu M, Honda S, Kirino Y. Dumbbell-PCR for Discriminative Quantification of a Small RNA Variant. *Methods Mol Biol*. 2018;1680:65-73
2. Honda S, Kirino Y. Dumbbell-PCR: a method to quantify specific small RNA variants with a single nucleotide resolution at terminal sequences. *Nucleic Acids Res*. 2015;43:e77
3. Mi H, Huang X, Muruganujan A, Tang H, Mills C, Kang D, Thomas PD. PANTHER version 11: expanded annotation data from Gene Ontology and Reactome pathways, and data analysis tool enhancements. *Nucleic Acids Res*. 2017;45:D183-D189